

# Bayesian updating of reliability by cross entropy-based importance sampling

Oindrila Kanjilal\*, Iason Papaioannou, Daniel Straub

*Engineering Risk Analysis Group, Technische Universität München, München 80290, Germany*

---

## Abstract

Bayesian analysis enables a consistent updating of the failure probability of engineering systems when new data is available. To this end, we introduce an adaptive importance sampling (IS) method based on the principle of cross entropy (CE) minimization. The key contribution is a novel IS density associated with the posterior probability density function (PDF) of the uncertain parameters, that facilitates efficient sampling from the important region of the failure domain, especially when the failure event is rare. The IS density is designed via a two-step procedure. The first step involves construction of a sample-based approximation of the posterior, which we build using the CE method. Here the aim is to determine the parameters of a chosen parametric distribution family that minimize its Kullback-Leibler divergence from the posterior PDF. The second step of the proposed method constructs the desired IS density for sampling the failure domain through a second round of CE minimization, starting from the approximate posterior obtained in the first step. An adaptive, multi-level approach is employed to solve the two CE optimization problems. The IS densities deduced in the two steps are then applied to construct an efficient estimator for the posterior probability of failure. Through numerical studies, we investigate and demonstrate the efficacy of the method in accurately estimating the reliability of engineering systems with rare failure events.

*Keywords:* Reliability updating, Bayesian analysis, Importance sampling, Cross entropy

---

## 1. Introduction

The prediction of reliability lies at the heart of model-based safety assessment of engineering systems. An accurate assessment requires appropriate characterization of the uncertain model parameters, taking into account all available data. Once an engineering system comes into existence, it is possible to obtain information on the system properties and performance through measurements, monitoring and other means of observations. This information can

---

\*Corresponding author

*Email addresses:* oindrila.kanjilal@tum.de (Oindrila Kanjilal), iason.papaioannou@tum.de (Iason Papaioannou), straub@tum.de (Daniel Straub)

7 be used to update the model parameters to provide improved estimates of the system's re-  
 8 liability. A consistent framework for assimilating the new information into the models is  
 9 provided by Bayesian analysis.

10 Consider the model,  $\mathcal{M}$ , of an engineering system, characterized by a set of model pa-  
 11 rameters and boundary conditions that describe the geometry, material properties, loads  
 12 etc. In many practical applications, some of these parameters are uncertain. Uncertain  
 13 parameters are modeled by random variables gathered in a random vector  $\Theta$  of dimension  
 14  $n_\theta$ . Let the probability density function (PDF)  $p_\Theta(\theta)$  denote one's prior belief about the  
 15 distribution of  $\Theta$ , i.e., before new information becomes available. The prior probability of  
 16 failure is given by the multi-dimensional integral

$$P_F = \int_{\theta \in \mathbb{R}^{n_\theta}} I_F(\theta) p_\Theta(\theta) d\theta, \quad (1)$$

17 where  $F = \{\theta \in \mathbb{R}^{n_\theta} : g(\theta) \leq 0\}$  is the failure event, defined in terms of the so called limit  
 18 state function  $g(\theta)$ , and  $I_F(\theta)$  is the indicator function such that  $I_F(\theta) = 1$  if  $g(\theta) \leq 0$   
 19 and  $I_F(\theta) = 0$  otherwise. Computation of the limit state function for an outcome  $\theta$  of the  
 20 uncertain parameters requires evaluation of the system model  $\mathcal{M}$ . The probability of the  
 21 complement of  $F$  is the reliability of the system.

22 When new data from the engineering system is available, it can be used to learn the  
 23 uncertain parameters, thereby updating the prior PDF. The data can be direct observations  
 24 of the uncertain parameters,  $\Theta$ , or measurements of the system response, e.g., measurements  
 25 of stress condition or deformation. Let  $\mathbf{d}$  denote the data that is available in the form of  
 26 measurements or observations. The updated/posterior PDF of  $\Theta$  that incorporates the data  
 27 information in the context of  $\mathcal{M}$  is given by Bayes' theorem as

$$p_{\Theta|\mathbf{d}}(\theta) = c_E^{-1} L(\theta|\mathbf{d}) p_\Theta(\theta). \quad (2)$$

28  $L(\theta|\mathbf{d})$  is the likelihood function that expresses the plausibility of observing  $\mathbf{d}$  given a certain  
 29  $\theta$  and  $c_E$  is the normalizing constant that ensures that  $p_{\Theta|\mathbf{d}}(\theta)$  integrates to one. It is  
 30 commonly referred to as the marginal likelihood (or evidence) and is defined as

$$c_E = \int_{\theta \in \mathbb{R}^{n_\theta}} L(\theta|\mathbf{d}) p_\Theta(\theta) d\theta. \quad (3)$$

31 When the data contains measurements of the system response,  $L(\theta|\mathbf{d})$  includes the system  
 32 model  $\mathcal{M}$  and Eq. (2) is termed a Bayesian inverse problem. The probability of failure  
 33 conditional on the data  $\mathbf{d}$  is obtained by replacing the prior PDF in Eq. (1) by the posterior  
 34 PDF

$$P_{F|\mathbf{d}} = \int_{\theta \in \mathbb{R}^{n_\theta}} I_F(\theta) p_{\Theta|\mathbf{d}}(\theta) d\theta \quad (4)$$

35 Evaluation of the posterior probability of failure requires repeated computation of the  
 36 limit state function and the likelihood over the outcome space of  $\Theta$ , and is challenging due to

37 several reasons. The functions  $L(\boldsymbol{\theta}|\mathbf{d})$  and  $g(\boldsymbol{\theta})$  are typically evaluated numerically, i.e., they  
38 are treated as black-box models. As a consequence, it is impossible to analytically evaluate  
39  $P_{F|\mathbf{d}}$  except for some special cases. Additionally, numerical integration of the integrals  
40 in Eqs. (3) and (4) is often not feasible due to the large number of random variables  
41 involved. Approaches to approximate the posterior probability of failure using the first- and  
42 second- order reliability methods [30] or Laplace’s asymptotic approximation [32] have been  
43 suggested. These methods require evaluations of the first and second derivatives of  $L(\boldsymbol{\theta}|\mathbf{d})$   
44 and  $g(\boldsymbol{\theta})$ , and, hence, might be computationally challenging, especially if the number of  
45 model parameters is large or evaluation of  $\mathcal{M}$  is costly. Moreover, they are often inaccurate  
46 in cases where the data is not informative.

47 Monte Carlo simulation (MCS) methods offer a robust alternative to numerically evaluate  
48  $P_{F|\mathbf{d}}$ . Here one can first perform a Bayesian analysis to learn the posterior PDF  $p_{\boldsymbol{\Theta}|\mathbf{d}}(\boldsymbol{\theta})$  of the  
49 uncertain parameters, and then use samples generated from  $p_{\boldsymbol{\Theta}|\mathbf{d}}(\boldsymbol{\theta})$  to evaluate  $P_{F|\mathbf{d}}$ . Beck  
50 and Au [5] propose an adaptive Metropolis-Hastings algorithm to generate samples from  
51  $p_{\boldsymbol{\Theta}|\mathbf{d}}(\boldsymbol{\theta})$  and then use these samples to update the reliability by evaluating the reliability  
52 conditional on each of these samples. This approach becomes inefficient when the number  
53 of uncertain model parameters  $n_{\boldsymbol{\theta}}$  is high and the posterior probability of failure is small.  
54 Ching and Hsieh [9] propose a method to update the reliability by combining Bayes’ theorem  
55 with maximum entropy theory. This approach uses standard MCS to fit a set of sampling  
56 distributions by the maximum entropy method. The method is suited for high dimensions  
57  $n_{\boldsymbol{\theta}}$ , but it remains inefficient for small target probabilities.

58 The limitation of the aforementioned simulation-based approaches in estimating small  
59 posterior failure probabilities can be overcome by combining the methods for Bayesian anal-  
60 ysis with advanced Monte Carlo methods for rare event estimation. Ching and Beck [7]  
61 propose a method for online reliability updating based on an efficient importance sampling  
62 technique of Au and Beck [2]. Sundar and Manohar [41] suggest an approach to estimate  
63 the posterior probability of failure by applying Girsanov’s transformation based importance  
64 sampling [29]. The methods in [7, 41] are applicable only if the system is dynamic and the  
65 model uncertainties are due to the unknown loading. Efficient approaches to update the reli-  
66 ability in the presence of both structural parameter and loading uncertainties are suggested  
67 in [21, 19, 4]. Jensen et al. [21] and Hadjidoukas et al. [19] propose to first update the  
68 prior PDF of the model parameters by applying the transitional Markov chain Monte Carlo  
69 method [8]. Subsequently, subset simulation [1] is employed for evaluating the conditional  
70 probability in Eq. (4) starting from samples of the posterior. The application of subset sim-  
71 ulation in conjunction with a Gibbs sampling-based method for Bayesian model updating  
72 [6] is explored in Bansal and Cheung [4]. Straub et al. [39, 40] present an approach that  
73 enables estimation of the updated failure probability without resorting to posterior samples.  
74 In this procedure, termed BUS (Bayesian updating with structural reliability methods), the  
75 integrals appearing in the definition of  $P_{F|\mathbf{d}}$  in Eq. (4) are converted into equivalent reliabil-  
76 ity integrals by means of appropriate transformations. These integrals can then be evaluated  
77 with any sampling-based reliability estimation method, such as importance sampling [39] or  
78 other advanced Monte Carlo techniques [33, 40]

79 In this contribution, we introduce a novel simulation-based method to update the re-

80 liability of engineering systems using data. The proposed procedure uses an importance  
81 sampling (IS) method that is developed based on the principle of cross entropy (CE) mini-  
82 mization. The key contribution is a novel IS density associated with the posterior PDF of  
83 the uncertain parameters, which facilitates efficient sampling of the important region of the  
84 failure domain, particularly for a small posterior probability of failure. The IS density is  
85 designed via a two-step procedure. The first step involves construction of a sample-based  
86 approximation of the posterior PDF, which we build using the CE method. Here the aim  
87 is to determine the parameters of a chosen parametric distribution family that minimize  
88 its Kullback-Leibler divergence from  $p_{\Theta|\mathbf{d}}(\boldsymbol{\theta})$ . The approximation leads to an efficient IS  
89 density for estimating the marginal likelihood. In the second step of the proposed method,  
90 we use the approximation of  $p_{\Theta|\mathbf{d}}(\boldsymbol{\theta})$  as a building block to construct the desired IS density  
91 for sampling the failure domain, through a second round of CE minimization. An adaptive,  
92 multi-level approach is employed to solve the CE optimization problem in each step. The  
93 IS densities deduced in the two steps are then applied to construct an efficient estimator for  
94 the posterior failure probability.

## 95 2. Importance sampling approach for reliability updating

96 The posterior probability of failure is defined in terms of the marginal likelihood,  $c_E$ , and  
97 the likelihood function,  $L(\boldsymbol{\theta}|\mathbf{d})$ , as

$$P_{F|\mathbf{d}} = \frac{1}{c_E} \int_{\boldsymbol{\theta} \in \mathbb{R}^{n_{\boldsymbol{\theta}}}} \mathbf{I}_F(\boldsymbol{\theta}) L(\boldsymbol{\theta}|\mathbf{d}) p_{\Theta}(\boldsymbol{\theta}) d\boldsymbol{\theta}. \quad (5)$$

98 One can evaluate  $P_{F|\mathbf{d}}$  by standard Monte Carlo simulation, via a rejection sampling scheme,  
99 wherein independent samples of the uncertain parameters  $\Theta$  generated from the prior PDF  
100 are used to estimate  $c_E$  and the posterior probability  $P_{F|\mathbf{d}}$ . When the posterior PDF of  
101  $\Theta$  differs significantly from the prior, or the failure event under the posterior probability  
102 measure is a rare event, this method requires a large number of samples to yield accurate  
103 estimates. A classical approach to address this drawback is to apply importance sampling.

104 Design of an efficient importance sampling scheme to evaluate the posterior probability  
105 of failure requires two main ingredients: (i) an IS density to estimate the marginal likelihood,  
106 and (ii) an IS density to integrate the un-normalized posterior PDF over the failure domain.  
107 Let  $q_{\Theta}^{(1)}(\boldsymbol{\theta})$  and  $q_{\Theta}^{(2)}(\boldsymbol{\theta})$  denote these two IS densities, respectively. Accordingly, Eq. (4) is  
108 written in the modified form

$$P_{F|\mathbf{d}} = \frac{1}{c_E} \int_{\boldsymbol{\theta} \in \mathbb{R}^{n_{\boldsymbol{\theta}}}} \mathbf{I}_F(\boldsymbol{\theta}) W_2(\boldsymbol{\theta}) q_{\Theta}^{(2)}(\boldsymbol{\theta}) d\boldsymbol{\theta}, \quad (6)$$

109 with

$$c_E = \int_{\boldsymbol{\theta} \in \mathbb{R}^{n_{\boldsymbol{\theta}}}} L(\boldsymbol{\theta}|\mathbf{d}) W_1(\boldsymbol{\theta}) q_{\Theta}^{(1)}(\boldsymbol{\theta}) d\boldsymbol{\theta}. \quad (7)$$

110 In the preceding equations,  $W_1(\boldsymbol{\theta}) = \frac{p_{\Theta}(\boldsymbol{\theta})}{q_{\Theta}^{(1)}(\boldsymbol{\theta})}$  and  $W_2(\boldsymbol{\theta}) = \frac{L(\boldsymbol{\theta}|\mathbf{d}) p_{\Theta}(\boldsymbol{\theta})}{q_{\Theta}^{(2)}(\boldsymbol{\theta})}$  are the importance

111 weight functions.

112 We develop an adaptive sampling strategy to determine the IS densities  $q_{\Theta}^{(1)}(\boldsymbol{\theta})$  and  
113  $q_{\Theta}^{(2)}(\boldsymbol{\theta})$ . The method is built on the principle of cross entropy (CE) minimization [36], a  
114 classical approach for constructing near-optimal IS densities for Monte Carlo integration.  
115 In the subsequent sections, we put forward a novel procedure to adapt this principle for the  
116 reliability updating problem. The proposed method is comprised of two steps. In the first  
117 step, described in Section 3, we determine the IS density  $q_{\Theta}^{(1)}(\boldsymbol{\theta})$ . We construct  $q_{\Theta}^{(1)}(\boldsymbol{\theta})$  as a  
118 near-optimal approximation of the posterior PDF,  $p_{\Theta|\mathbf{d}}(\boldsymbol{\theta})$ . We adopt the approach devel-  
119 oped in our recent work [15], where we approximate  $p_{\Theta|\mathbf{d}}(\boldsymbol{\theta})$  by a parametric density that  
120 minimizes the cross entropy (CE) loss between  $p_{\Theta|\mathbf{d}}(\boldsymbol{\theta})$  and a chosen family of parametric  
121 distributions. In the next step, we construct  $q_{\Theta}^{(2)}(\boldsymbol{\theta})$  as an approximation of the optimal IS  
122 density for integrating the un-normalized posterior PDF over the failure domain. The pro-  
123 cedure requires a second round of CE minimization. The approach, developed in Section 4,  
124 leverages upon the approximation of  $p_{\Theta|\mathbf{d}}(\boldsymbol{\theta})$  of the first step, and a smooth approximation  
125 of the indicator of the failure event, used earlier by [34, 35], to efficiently solve the CE opti-  
126 mization problem. We provide the proposed IS estimator of the posterior failure probability  
127 and discuss its statistical properties. In Section 5, we discuss the choice of the parametric  
128 density in the CE method, which is followed by numerical investigations in Section 6 that  
129 demonstrate the performance of our method.

### 130 3. Approximation of the posterior PDF

131 As already noted, it is straightforward to evaluate the marginal likelihood,  $c_E$ , by stan-  
132 dard Monte Carlo simulation (MCS): one generates independent samples  $\{\boldsymbol{\theta}^{(i)}, i = 1, \dots, N_1\}$   
133 from the prior PDF  $p_{\Theta}(\boldsymbol{\theta})$  and computes the sample mean of the likelihood function values  
134  $\{L(\boldsymbol{\theta}^{(i)}|\mathbf{d}), i = 1, \dots, N_1\}$ . However, if the data is highly informative, the posterior PDF  
135 tends to differ significantly from the prior PDF, necessitating a very large number of sam-  
136 ples  $N_1$  to obtain an accurate estimate, i.e., an estimate with a small coefficient of variation  
137 (CoV). Importance sampling provides a path to overcome the drawback of standard MCS.  
138 The IS density should be selected such that the IS estimator has a smaller coefficient of  
139 variation (CoV) compared to the estimator in standard Monte Carlo. Following (7), one  
140 can show that if the posterior PDF is selected as the IS density, i.e., if  $q_{\Theta}^{(1)}(\boldsymbol{\theta}) = p_{\Theta|\mathbf{d}}(\boldsymbol{\theta})$ ,  
141 the CoV of the IS estimator of the marginal likelihood reduces to zero. In the context of  
142 importance sampling, such a density is termed the optimal IS density [36]. The optimal IS  
143 density  $p_{\Theta|\mathbf{d}}(\boldsymbol{\theta})$  requires knowledge of the target quantity  $c_E$ , and hence cannot be directly  
144 applied. However, it is possible to construct an IS density that closely resembles  $p_{\Theta|\mathbf{d}}(\boldsymbol{\theta})$ ,  
145 and subsequently apply it to estimate  $c_E$ . In [15], we construct an approximation of the  
146 posterior PDF by fitting parametric density models using the CE method. The approach is  
147 summarized in the following.

148 *3.1. Multi-level cross entropy method for posterior approximation*

149 Consider a family of parametric densities  $q_{\Theta}(\boldsymbol{\theta}; \boldsymbol{\nu})$  defined by the parameter vector  $\boldsymbol{\nu} \in \mathcal{V}$ .  
 150 We select  $q_{\Theta}(\boldsymbol{\theta}; \boldsymbol{\nu})$  such that it contains the prior PDF of the uncertain parameters, i.e.,  
 151  $q_{\Theta}(\boldsymbol{\theta}; \hat{\boldsymbol{\nu}}_0) = p_{\Theta}(\boldsymbol{\theta})$  for  $\hat{\boldsymbol{\nu}}_0 \in \mathcal{V}$ . The choice of the family  $q_{\Theta}(\boldsymbol{\theta}; \boldsymbol{\nu})$  is detailed in Section 5.  
 152 The CE method aims at constructing a near-optimal IS density by minimizing the Kullback-  
 153 Leibler (KL) divergence between the optimal IS density and the chosen parametric family  
 154 [36]. The KL divergence between  $p_{\Theta|\mathbf{d}}(\boldsymbol{\theta})$  and  $q_{\Theta}(\boldsymbol{\theta}; \boldsymbol{\nu})$  is a measure of distance between the  
 155 two PDFs and is defined as

$$\begin{aligned} D_{KL}(p_{\Theta|\mathbf{d}}(\boldsymbol{\theta})||q_{\Theta}(\boldsymbol{\theta}; \boldsymbol{\nu})) &= \mathbb{E}_{p_{\Theta|\mathbf{d}}} \left[ \ln \left( \frac{p_{\Theta|\mathbf{d}}(\boldsymbol{\theta})}{q_{\Theta}(\boldsymbol{\theta}; \boldsymbol{\nu})} \right) \right] \\ &= \frac{1}{c_E} \mathbb{E}_{p_{\Theta}} [L(\boldsymbol{\theta}|\mathbf{d}) \ln(p_{\Theta|\mathbf{d}}(\boldsymbol{\theta}))] - \frac{1}{c_E} \mathbb{E}_{p_{\Theta}} [L(\boldsymbol{\theta}|\mathbf{d}) \ln(q_{\Theta}(\boldsymbol{\theta}; \boldsymbol{\nu}))] \end{aligned} \quad (8)$$

156 Since the first expectation on the right-hand side of Eq. (8) is not a function of  $\boldsymbol{\nu}$ , minimizing  
 157  $D_{KL}(p_{\Theta|\mathbf{d}}(\boldsymbol{\theta})||q_{\Theta}(\boldsymbol{\theta}; \boldsymbol{\nu}))$  is equivalent to solving the stochastic optimization problem:

$$\boldsymbol{\nu}_{c_E}^* = \underset{\boldsymbol{a} \in \mathcal{V}}{\operatorname{argmax}} \mathbb{E}_{p_{\Theta}} [L(\boldsymbol{\theta}|\mathbf{d}) \ln(q_{\Theta}(\boldsymbol{\theta}; \boldsymbol{a}))] \quad (9)$$

158 The parametric density defined by  $\boldsymbol{\nu}_{c_E}^*$  is a near-optimal approximation of the posterior PDF  
 159  $p_{\Theta|\mathbf{d}}(\boldsymbol{\theta})$ . The above optimization can be solved by approximating the expectation in Eq. (9)  
 160 with a set of samples drawn from  $p_{\Theta}(\boldsymbol{\theta})$ . However, the number of samples required to obtain  
 161 a good sample approximation is large when  $p_{\Theta|\mathbf{d}}(\boldsymbol{\theta})$  differs significantly from  $p_{\Theta}(\boldsymbol{\theta})$ . In such  
 162 cases, directly solving Eq. (9) is computationally challenging. To address this challenge, in  
 163 [15] we develop a multi-level version of the CE method that approaches the target density  
 164  $p_{\Theta|\mathbf{d}}(\boldsymbol{\theta})$  step-wise through a sequence of parametric densities defined by  $\{\boldsymbol{\nu}_k, k = 1, \dots, L_1\}$ .

165 We consider a sequence of intermediate target densities  $\{h_1^k(\boldsymbol{\theta}), k = 0, \dots, L_1\}$  that  
 166 starts from the prior PDF  $p_{\Theta}(\boldsymbol{\theta})$  and gradually approaches the posterior PDF  $p_{\Theta|\mathbf{d}}(\boldsymbol{\theta})$ . The  
 167 distribution sequence is constructed by tempering the likelihood function (i.e., by taking it  
 168 to be the power of  $\gamma_k$ ):

$$h_1^k(\boldsymbol{\theta}) = \frac{1}{C_k} L(\boldsymbol{\theta}|\mathbf{d})^{\gamma_k} p_{\Theta}(\boldsymbol{\theta}). \quad (10)$$

169 Here  $C_k$  is the normalizing constant of  $h_1^k(\boldsymbol{\theta})$  and  $0 = \gamma_0 < \gamma_1 < \dots < \gamma_{L_1} = 1$  are  
 170 tempering parameters which ensure a smooth transition between the prior and posterior  
 171 PDFs of  $\Theta$ . Note that  $h_1^0(\boldsymbol{\theta}) = p_{\Theta}(\boldsymbol{\theta})$  and  $h_1^{L_1}(\boldsymbol{\theta}) = p_{\Theta|\mathbf{d}}(\boldsymbol{\theta})$ . This distribution sequence  
 172 has been used in [31, 10, 8] to design Markov chain-based sequential Monte Carlo samplers  
 173 for Bayesian analysis. We approach the posterior PDF  $p_{\Theta|\mathbf{d}}(\boldsymbol{\theta})$  gradually, by solving the  
 174 CE optimization problem sequentially for each intermediate target density. This leads to  
 175 a sequence of parameter vectors  $\{\boldsymbol{\nu}_k, k = 1, \dots, L_1\}$  such that the final parameter  $\boldsymbol{\nu}_{L_1}$  is a  
 176 good approximation of the optimal parameter  $\boldsymbol{\nu}_{c_E}^*$ . We determine  $\boldsymbol{\nu}_k$  by minimizing the KL  
 177 divergence between  $h_1^k(\boldsymbol{\theta})$  and  $q_{\Theta}(\boldsymbol{\theta}; \boldsymbol{\nu})$ :

$$\begin{aligned}
\boldsymbol{\nu}_k &= \underset{\mathbf{a} \in \mathcal{V}}{\operatorname{argmin}} D_{KL} (h_1^k(\boldsymbol{\theta}) || q_{\Theta}(\boldsymbol{\theta}; \boldsymbol{\nu})) \\
&= \underset{\mathbf{a} \in \mathcal{V}}{\operatorname{argmax}} E_{p_{\Theta}} [L(\boldsymbol{\theta}|\mathbf{d})^{\gamma_k} \ln (q_{\Theta}(\boldsymbol{\theta}; \mathbf{a}))]
\end{aligned} \tag{11}$$

178 The objective function of the corresponding optimization problem, i.e., the expectation  
179  $E_{p_{\Theta}} [L(\boldsymbol{\theta}|\mathbf{d})^{\gamma_k} \ln (q_{\Theta}(\boldsymbol{\theta}; \mathbf{a}))]$ , is approximated by importance sampling using a set of samples  
180  $\{\boldsymbol{\theta}^{(i)}, i = 1, \dots, N\}$  distributed according to  $q_{\Theta}(\boldsymbol{\theta}; \hat{\boldsymbol{\nu}}_{k-1})$ , where  $\hat{\boldsymbol{\nu}}_{k-1}$  is the estimate of  $\boldsymbol{\nu}_{k-1}$   
181 determined in the previous level. At  $k = 0$ , the sampling density  $q_{\Theta}(\boldsymbol{\theta}; \hat{\boldsymbol{\nu}}_0)$  corresponds to  
182 the prior PDF  $p_{\Theta}(\boldsymbol{\theta})$ . This leads to the following stochastic optimization problem to be  
183 solved in each intermediate level :

$$\hat{\boldsymbol{\nu}}_k = \underset{\mathbf{a} \in \mathcal{V}}{\operatorname{argmax}} \frac{1}{N} \sum_{i=1}^N \widetilde{W}_k^1(\boldsymbol{\theta}^{(i)}, \hat{\boldsymbol{\nu}}_{k-1}) \ln (q_{\Theta}(\boldsymbol{\theta}^{(i)}; \mathbf{a})), \tag{12}$$

184 where  $\widetilde{W}_k^1(\boldsymbol{\theta}^{(i)}, \hat{\boldsymbol{\nu}}_{k-1}) = L(\boldsymbol{\theta}^{(i)}|\mathbf{d})^{\gamma_k} \frac{p_{\Theta}(\boldsymbol{\theta}^{(i)})}{q_{\Theta}(\boldsymbol{\theta}^{(i)}; \hat{\boldsymbol{\nu}}_{k-1})}$  is the importance weight of a sample  $\boldsymbol{\theta}^{(i)}$ .

185 The accuracy and computational cost of this procedure depends on the choice of the  
186 tempering parameters  $\{\gamma_k, k = 1, \dots, L_1\}$ , which determine the change between the respec-  
187 tive target densities. In order to obtain a good estimate of  $\hat{\boldsymbol{\nu}}_k$  with a limited number of  
188 samples, the intermediate PDF  $h_1^k(\boldsymbol{\theta})$  should not differ largely from the parametric density  
189  $q_{\Theta}(\boldsymbol{\theta}; \hat{\boldsymbol{\nu}}_{k-1})$ . To ensure this, we adopt the criterion suggested in [34] and select the tem-  
190 pering parameter  $\gamma_k$  adaptively, on the fly, such that the sample CoV  $\hat{\delta}_{\widetilde{W}_k^1}$  of the weights  
191  $\{\widetilde{W}_k^1(\boldsymbol{\theta}^{(i)}), i = 1, \dots, N\}$  adheres to a target value  $\delta_{\gamma}^* = 1.5$ :

$$\gamma_k = \underset{\gamma \in (\gamma_{k-1}, 1)}{\operatorname{argmin}} \left( \hat{\delta}_{\widetilde{W}_k^1}(\gamma) - \delta_{\gamma}^* \right)^2. \tag{13}$$

192 The adaptive procedure terminates when the value of  $\gamma_k$  determined based on Eq. (13)  
193 equals 1. After termination, the final parameter vector  $\hat{\boldsymbol{\nu}}_{L_1}$  is determined by solving Eq.  
194 (12) with  $\gamma_{L_1} = 1$ .  $\hat{\boldsymbol{\nu}}_{L_1}$  closely approximates the optimal parameter  $\boldsymbol{\nu}_{cE}^*$  in Eq. (9). Thus,  
195  $q_{\Theta}(\boldsymbol{\theta}; \hat{\boldsymbol{\nu}}_{L_1})$  is a close approximation of the posterior PDF for the chosen parametric family,  
196 and is taken as the IS density for estimating the marginal likelihood,  $c_E$ .

#### 197 4. Estimation of the posterior probability of failure

198 The parametric density  $q_{\Theta}(\boldsymbol{\theta}; \hat{\boldsymbol{\nu}}_{L_1})$  describing the posterior PDF could be applied to  
199 estimate the posterior probability of failure by importance sampling. However, if the failure  
200 event,  $F$ , is rare under the posterior probability measure, the samples from  $q_{\Theta}(\boldsymbol{\theta}; \hat{\boldsymbol{\nu}}_{L_1})$  do  
201 not represent well the failure domain, resulting in a high sampling CoV of the associated IS  
202 estimator. In contrast, the optimal IS density that perfectly describes  $F$ , and leads to an IS  
203 estimator with sampling CoV equal to zero, is given by

$$q_{P_{F|d}}^*(\boldsymbol{\theta}) = \frac{1}{P_{F|d}} I_F(\boldsymbol{\theta}) p_{\Theta|d}(\boldsymbol{\theta}). \quad (14)$$

204 The above IS density, however, cannot be applied in practice, as it requires knowledge of the  
 205 target probability of failure. We develop an extension of the multi-level CE method described  
 206 in the previous section, to construct an IS density  $q_{\Theta}^{(2)*}(\boldsymbol{\theta})$  that is a close approximation of  
 207 the optimal IS density  $q_{P_{F|d}}^*(\boldsymbol{\theta})$ . The proposed IS density is able to adequately describe the  
 208 rare failure region, and, together with  $q_{\Theta}(\boldsymbol{\theta}; \hat{\boldsymbol{\nu}}_{L_1})$ , it leads to an efficient IS estimator for the  
 209 posterior failure probability.

210 Consider the parametric density family  $q_{\Theta}(\boldsymbol{\theta}; \boldsymbol{\nu}); \boldsymbol{\nu} \in \mathcal{V}$  introduced in the previous sec-  
 211 tion. An approximation of the optimal IS density  $q_{P_{F|d}}^*(\boldsymbol{\theta})$  is deduced by the CE method,  
 212 by minimizing the KL divergence between  $q_{P_{F|d}}^*(\boldsymbol{\theta})$  and  $q_{\Theta}(\boldsymbol{\theta}; \boldsymbol{\nu})$ , i.e., by solving the CE  
 213 optimization problem

$$\begin{aligned} \boldsymbol{\nu}_{P_{F|d}}^* &= \operatorname{argmin}_{\boldsymbol{\nu} \in \mathcal{V}} D_{KL} \left( q_{P_{F|d}}^*(\boldsymbol{\theta}) \parallel q_{\Theta}(\boldsymbol{\theta}; \boldsymbol{\nu}) \right) \\ &= \operatorname{argmax}_{\boldsymbol{\nu} \in \mathcal{V}} \mathbb{E}_{p_{\Theta|d}} [I_F(\boldsymbol{\theta}) \ln (q_{\Theta}(\boldsymbol{\theta}; \boldsymbol{\nu}))]. \end{aligned} \quad (15)$$

214 One can solve the above optimization in a single step, after approximating the expectation  
 215 through importance sampling using samples from the parametric density  $q_{\Theta}(\boldsymbol{\theta}; \hat{\boldsymbol{\nu}}_{L_1})$  describ-  
 216 ing the posterior PDF,  $p_{\Theta|d}(\boldsymbol{\theta})$ . This approach, however, requires a large number of samples  
 217 when the failure event is rare. By analogy with Section 3, we lay out a multi-level procedure  
 218 that approaches the target density  $q_{P_{F|d}}^*(\boldsymbol{\theta})$  step-wise, by approximating a sequence of target  
 219 densities  $\{h_2^k(\boldsymbol{\theta}), k = 1, \dots, L_2\}$  residing between the posterior PDF  $p_{\Theta|d}(\boldsymbol{\theta})$  and  $q_{P_{F|d}}^*(\boldsymbol{\theta})$ .  
 220 The approach, described in Section 4.1, results in an extended sequence of parameter vectors  
 221  $\{\hat{\boldsymbol{\nu}}_{k+L_1}, k = 1, \dots, L_2\}$  where the final parameter  $\hat{\boldsymbol{\nu}}_{L_2+L_1}$  is a good approximation of  $\boldsymbol{\nu}_{P_{F|d}}^*$ .  
 222 The parametric density  $q_{\Theta}(\boldsymbol{\theta}; \hat{\boldsymbol{\nu}}_{L_2+L_1})$ , which is close to the optimal IS density  $q_{P_{F|d}}^*(\boldsymbol{\theta})$ , is  
 223 then applied to estimate the posterior probability of failure by importance sampling.

#### 224 4.1. Multi-level CE method for estimation of the posterior failure probability

225 In the standard multi-level CE method for rare event estimation [36], the intermediate  
 226 target densities correspond to the optimal IS densities of intermediate reliability integrals,  
 227 defined by a sequence of failure events that gradually approach the rare failure event  $F$ . To  
 228 enable better use of the samples generated at each level, Papaioannou et al. [35] proposed to  
 229 characterize the intermediate densities using a smooth approximation of  $I_F(\boldsymbol{\theta})$  based on the  
 230 standard normal cumulative distribution function  $\Phi(\cdot)$ . We follow the distribution sequence  
 231 suggested in [35] and define the intermediate target densities for estimating the posterior  
 232 failure probability as

$$h_2^k(\boldsymbol{\theta}) = \frac{1}{P_k} \Phi \left( -\frac{g(\boldsymbol{\theta})}{\sigma_k} \right) p_{\Theta|d}(\boldsymbol{\theta}), \quad (16)$$

233 where  $\sigma_1 > \sigma_2 > \dots > \sigma_{L_2} > 0$  are smoothing parameters and  $P_k$  is the normalizing constant

234 of  $h_2^k(\boldsymbol{\theta})$ . Note that  $\lim_{\sigma \rightarrow 0} \Phi\left(-\frac{g(\boldsymbol{\theta})}{\sigma}\right) = \mathbb{I}\{g(\boldsymbol{\theta}) \leq 0\}$ . Hence, with decreasing  $\sigma$ , the above  
 235 sequence converges to the optimal IS density  $q_{P_{F|\mathbf{d}}}^*(\boldsymbol{\theta})$  in Eq. (14).

236 Starting from the parametric density  $q_{\Theta}(\boldsymbol{\theta}; \hat{\boldsymbol{\nu}}_{L_1})$  approximating the posterior PDF  $p_{\Theta|\mathbf{d}}(\boldsymbol{\theta})$ ,  
 237 we construct a sequence of densities  $\{q_{\Theta}(\boldsymbol{\theta}; \boldsymbol{\nu}_{k+L_1}), k = 1, \dots, L_2\}$  such that  $q_{\Theta}(\boldsymbol{\theta}; \boldsymbol{\nu}_{k+L_1})$   
 238 has the minimum KL divergence from  $h_2^k(\boldsymbol{\theta})$  within the parametric family. The parameter  
 239 vector  $\hat{\boldsymbol{\nu}}_{k+L_1}$  is determined by solving the sample counter-part of the CE optimization:

$$\boldsymbol{\nu}_{k+L_1} = \operatorname{argmax}_{\mathbf{a} \in \mathcal{V}} \mathbb{E}_{p_{\Theta|\mathbf{d}}} \left[ \Phi\left(-\frac{g(\boldsymbol{\theta})}{\sigma_k}\right) \ln(q_{\Theta}(\boldsymbol{\theta}; \mathbf{a})) \right]. \quad (17)$$

240 We approximate the expectation in Eq. (17) through importance sampling using samples  
 241  $\{\boldsymbol{\theta}^{(i)}, i = 1, \dots, N\}$  generated from  $q_{\Theta}(\boldsymbol{\theta}; \hat{\boldsymbol{\nu}}_{k+L_1-1})$ , to arrive at the following optimization  
 242 problem:

$$\hat{\boldsymbol{\nu}}_{k+L_1} = \operatorname{argmax}_{\mathbf{a} \in \mathcal{V}} \sum_{i=1}^N \widetilde{W}_k^2(\boldsymbol{\theta}^{(i)}, \hat{\boldsymbol{\nu}}_{k+L_1-1}) \ln(q_{\Theta}(\boldsymbol{\theta}^{(i)}; \mathbf{a})), \quad (18)$$

243 with  $\widetilde{W}_k^2(\boldsymbol{\theta}; \hat{\boldsymbol{\nu}}_{k+L_1-1}) = \Phi\left(-\frac{g(\boldsymbol{\theta})}{\sigma_k}\right) \frac{L(\boldsymbol{\theta}|\mathbf{d})p_{\Theta}(\boldsymbol{\theta})}{q_{\Theta}(\boldsymbol{\theta}; \hat{\boldsymbol{\nu}}_{k+L_1-1})}$ . To ensure that a good estimate of  $\boldsymbol{\nu}_{k+L_1}$   
 244 is obtained with a reasonable number of samples drawn from  $q_{\Theta}(\boldsymbol{\theta}; \hat{\boldsymbol{\nu}}_{k+L_1-1})$ , in each level the  
 245 smoothing parameter is selected such that the sample CoV  $\hat{\delta}_{\widetilde{W}_k^2}$  of the weights  $\left\{ \widetilde{W}_k^2(\boldsymbol{\theta}^{(i)}, \hat{\boldsymbol{\nu}}_{k+L_1-1}), i = 1, \dots, N \right\}$ ,  
 246 adheres to a target value  $\delta_{\sigma}^*$ :

$$\sigma_k = \operatorname{argmin}_{\sigma \in (0, \sigma_{k-1})} \left( \hat{\delta}_{\widetilde{W}_k^2}(\sigma) - \delta_{\sigma}^* \right)^2. \quad (19)$$

247 We select  $\delta_{\sigma}^* = 1.5$  [34]. The adaptive procedure terminates when the CoV of the weights of  
 248 the current smooth approximation with respect to the optimal IS density  $\left\{ \frac{\mathbb{I}\{g(\boldsymbol{\theta}^{(i)}) \leq 0\}}{\Phi\left(-\frac{g(\boldsymbol{\theta}^{(i)})}{\sigma_k}\right)}, i = 1, \dots, N \right\}$   
 249 is smaller than  $\delta_{\sigma}^*$ .

#### 250 4.2. Estimator for the posterior probability of failure

251 The fitted IS density  $q_{\Theta}(\boldsymbol{\theta}; \hat{\boldsymbol{\nu}}_{L_2+L_1})$  is applied to evaluate the posterior probability of  
 252 failure by importance sampling. Accordingly, we write Eq. (4) in the modified form

$$\begin{aligned} P_{F|\mathbf{d}} &= \int_{\boldsymbol{\theta} \in \mathbb{R}^{n_{\boldsymbol{\theta}}}} \mathbb{I}_F(\boldsymbol{\theta}) \frac{p_{\Theta|\mathbf{d}}(\boldsymbol{\theta})}{q_{\Theta}(\boldsymbol{\theta}; \hat{\boldsymbol{\nu}}_{L_2+L_1})} q_{\Theta}(\boldsymbol{\theta}; \hat{\boldsymbol{\nu}}_{L_2+L_1}) d\boldsymbol{\theta} \\ &= \frac{1}{c_E} \int_{\boldsymbol{\theta} \in \mathbb{R}^{n_{\boldsymbol{\theta}}}} \mathbb{I}_F(\boldsymbol{\theta}) \frac{L(\boldsymbol{\theta}|\mathbf{d})p_{\Theta}(\boldsymbol{\theta})}{q_{\Theta}(\boldsymbol{\theta}; \hat{\boldsymbol{\nu}}_{L_2+L_1})} q_{\Theta}(\boldsymbol{\theta}; \hat{\boldsymbol{\nu}}_{L_2+L_1}) d\boldsymbol{\theta}. \end{aligned} \quad (20)$$

253 The marginal likelihood,  $c_E$ , is evaluated by importance sampling using the IS density

254  $q_{\Theta}(\boldsymbol{\theta}; \hat{\boldsymbol{\nu}}_{L_1})$ . This leads to

$$P_{F|\mathbf{d}} = \frac{\int_{\boldsymbol{\theta} \in \mathbb{R}^{n_{\boldsymbol{\theta}}}} \mathbf{I}_F(\boldsymbol{\theta}) W_2(\boldsymbol{\theta}) q_{\Theta}(\boldsymbol{\theta}; \hat{\boldsymbol{\nu}}_{L_2+L_1}) d\boldsymbol{\theta}}{\int_{\boldsymbol{\theta} \in \mathbb{R}^{n_{\boldsymbol{\theta}}}} L(\boldsymbol{\theta}|\mathbf{d}) W_1(\boldsymbol{\theta}) q_{\Theta}(\boldsymbol{\theta}; \hat{\boldsymbol{\nu}}_{L_1}) d\boldsymbol{\theta}}, \quad (21)$$

255 where  $W_1(\boldsymbol{\theta}) = \frac{p_{\Theta}(\boldsymbol{\theta})}{q_{\Theta}(\boldsymbol{\theta}; \hat{\boldsymbol{\nu}}_{L_1})}$  and  $W_2(\boldsymbol{\theta}) = \frac{L(\boldsymbol{\theta}|\mathbf{d}) p_{\Theta}(\boldsymbol{\theta})}{q_{\Theta}(\boldsymbol{\theta}; \hat{\boldsymbol{\nu}}_{L_2+L_1})}$  are IS weights. The corresponding  
256 estimator is

$$\hat{P}_{F|\mathbf{d}}^{\text{IS}} = \frac{\frac{1}{N_{\text{IS},2}} \sum_{i=1}^{N_{\text{IS},2}} \mathbf{I}_F(\boldsymbol{\theta}^{(2,i)}) W_2(\boldsymbol{\theta}^{(2,i)})}{\frac{1}{N_{\text{IS},1}} \sum_{i=1}^{N_{\text{IS},1}} L(\boldsymbol{\theta}^{(1,i)}|\mathbf{d}) W_1(\boldsymbol{\theta}^{(1,i)})}, \quad (22)$$

257 where  $\{\boldsymbol{\theta}^{(1,i)}, i = 1, \dots, N_{\text{IS},1}\}$  and  $\{\boldsymbol{\theta}^{(2,i)}, i = 1, \dots, N_{\text{IS},2}\}$  are independent samples gener-  
258 ated from the IS densities  $q_{\Theta}(\boldsymbol{\theta}; \hat{\boldsymbol{\nu}}_{L_1})$  and  $q_{\Theta}(\boldsymbol{\theta}; \hat{\boldsymbol{\nu}}_{L_2+L_1})$ , respectively.

#### 259 4.3. Statistics of the proposed estimator

260 The bias and CoV of the estimator of the posterior failure probability are given by the  
261 following two propositions. We denote the estimators in the denominator and numerator of  
262 Eq. (22) by  $\hat{P}_1$  and  $\hat{P}_2$ , respectively. Let  $P_1$  and  $P_2$ , respectively, denote the true values of  
263  $\hat{P}_1$  and  $\hat{P}_2$ , i.e.,  $P_{F|\mathbf{d}} = \frac{P_2}{P_1}$ . For simplicity we set  $N_{\text{IS},1} = N_{\text{IS},2} = N$ .

264 **Proposition 1.**  $\hat{P}_{F|\mathbf{d}}^{\text{IS}}$  is biased for finite  $N$ . The fractional bias is given by:  
265

$$\mathbb{E} \left[ \frac{\hat{P}_{F|\mathbf{d}}^{\text{IS}} - P_{F|\mathbf{d}}}{P_{F|\mathbf{d}}} \right] = \delta_1^2 - \rho_{12} \delta_1 \delta_2 + o(1/N) = O(1/N), \quad (23)$$

266 where  $\delta_1$  and  $\delta_2$ , respectively, denote the CoV of  $\hat{P}_1$  and  $\hat{P}_2$ , and  $\rho_{12}$  denotes the correlation  
267 coefficient between the estimators.  $\hat{P}_{F|\mathbf{d}}^{\text{IS}}$  is thus asymptotically unbiased and the bias is  
268  $O(1/N)$ .

269 **Proof.** Since  $\hat{P}_{F|\mathbf{d}}^{\text{IS}} = \frac{\hat{P}_2}{\hat{P}_1}$  and  $P_{F|\mathbf{d}} = \frac{P_2}{P_1}$ , it follows that  
270

$$\frac{\hat{P}_{F|\mathbf{d}}^{\text{IS}} - P_{F|\mathbf{d}}}{P_{F|\mathbf{d}}} = \left( \frac{\hat{P}_2}{P_2} - \frac{\hat{P}_1}{P_1} \right) \frac{P_1}{\hat{P}_1}. \quad (24)$$

271 Taylor series expansion of  $\frac{P_1}{\hat{P}_1}$  around  $P_1$  leads to

$$\begin{aligned} \frac{\hat{P}_{F|\mathbf{d}}^{\text{IS}} - P_{F|\mathbf{d}}}{P_{F|\mathbf{d}}} &= \left( \frac{\hat{P}_2}{P_2} - \frac{\hat{P}_1}{P_1} \right) \left( 1 - \frac{\hat{P}_1 - P_1}{P_1} + \left( \frac{\hat{P}_1 - P_1}{P_1} \right)^2 + \dots \right) \\ &= \frac{\hat{P}_2}{P_2} - \frac{\hat{P}_1}{P_1} + \frac{\hat{P}_1 (\hat{P}_1 - P_1)}{P_1^2} - \frac{\hat{P}_2 (\hat{P}_1 - P_1)}{P_1 P_2} + \dots \end{aligned} \quad (25)$$

272 Taking expectation on both sides of Eq. (25) and noting that the estimators  $\hat{P}_1$  and  $\hat{P}_2$  are  
 273 unbiased, i.e.,  $E[\hat{P}_1] = P_1$  and  $E[\hat{P}_2] = P_2$ , proves the required proposition.  $\square$

274

275 **Proposition 2.** The CoV  $\delta_{\hat{P}_{F|\mathbf{d}}^{\text{IS}}}$  of  $\hat{P}_{F|\mathbf{d}}^{\text{IS}}$  is given by:

$$\delta_{\hat{P}_{F|\mathbf{d}}^{\text{IS}}}^2 = E \left[ \frac{\hat{P}_{F|\mathbf{d}}^{\text{IS}} - P_{F|\mathbf{d}}}{P_{F|\mathbf{d}}} \right]^2 = \delta_1^2 + \delta_2^2 - \rho_{12}\delta_1\delta_2 + o(1/N) = O(1/N) \quad (26)$$

276 where  $\delta_1$  and  $\delta_2$ , respectively, denote the CoV of  $\hat{P}_1$  and  $\hat{P}_2$ , and  $\rho_{12}$  denotes the correlation  
 277 coefficient between the estimators.  $\hat{P}_{F|\mathbf{d}}^{\text{IS}}$  is thus a consistent estimator and its CoV  $\delta_{\hat{P}_{F|\mathbf{d}}^{\text{IS}}}$  is  
 278  $O(1/\sqrt{N})$ .

279

280 **Proof.** From Eq. (25)

$$\begin{aligned} E \left[ \frac{\hat{P}_{F|\mathbf{d}}^{\text{IS}} - P_{F|\mathbf{d}}}{P_{F|\mathbf{d}}} \right]^2 &= E \left[ \frac{\hat{P}_2}{P_2} - \frac{\hat{P}_1}{P_1} + \frac{\hat{P}_1 (\hat{P}_1 - P_1)}{P_1^2} - \frac{\hat{P}_2 (\hat{P}_1 - P_1)}{P_1 P_2} + \dots \right]^2 \\ &= E \left[ \frac{\hat{P}_2 - P_2}{P_2} - \frac{\hat{P}_1 - P_1}{P_1} + \frac{\hat{P}_1 (\hat{P}_1 - P_1)}{P_1^2} - \frac{\hat{P}_2 (\hat{P}_1 - P_1)}{P_1 P_2} + \dots \right]^2 \\ &= E \left[ \frac{\hat{P}_1 - P_1}{P_1} \right]^2 + E \left[ \frac{\hat{P}_2 - P_2}{P_2} \right]^2 - E \left[ \left( \frac{\hat{P}_1 - P_1}{P_1} \right) \left( \frac{\hat{P}_2 - P_2}{P_2} \right) \right] + o \left( \frac{1}{N} \right) \end{aligned} \quad (27)$$

281 Hence the proposition.  $\square$

282 In practice, it is reasonable to assume that the estimators  $\hat{P}_1$  and  $\hat{P}_2$  are uncorrelated.  
 283 Then, we can use the first two terms on the R.H.S of Eq. (26) to obtain an approximate  
 284 estimate of the CoV of the probability of failure estimator:

$$\hat{\delta}_{\hat{P}_{F|\mathbf{d}}^{\text{IS}}}^2 \approx \hat{\delta}_1^2 + \hat{\delta}_2^2, \quad (28)$$

285 where  $\hat{\delta}_{\hat{P}_{F|\mathbf{d}}^{\text{IS}}}$ ,  $\hat{\delta}_1$  and  $\hat{\delta}_2$  denote sample estimates of  $\delta_{\hat{P}_{F|\mathbf{d}}^{\text{IS}}}$ ,  $\delta_1$  and  $\delta_2$ , respectively. The estimates  
 286 of  $\delta_1$  and  $\delta_2$  are obtained according to [28]

$$\hat{\delta}_1^2 = \frac{1}{\hat{P}_1^2} \frac{1}{N_{\text{IS},1} - 1} \left[ \frac{1}{N_{\text{IS},1}} \sum_{i=1}^{N_{\text{IS},1}} \left\{ L(\boldsymbol{\theta}^{(1,i)}|\mathbf{d}) W_1(\boldsymbol{\theta}^{(1,i)}) \right\}^2 - \hat{P}_1^2 \right] \quad (29)$$

287 and

$$\hat{\delta}_2^2 = \frac{1}{\hat{P}_2^2} \frac{1}{N_{\text{IS},2} - 1} \left[ \frac{1}{N_{\text{IS},2}} \sum_{i=1}^{N_{\text{IS},2}} I_F(\boldsymbol{\theta}^{(2,i)}) \left\{ W_2(\boldsymbol{\theta}^{(2,i)}) \right\}^2 - \hat{P}_2^2 \right]. \quad (30)$$

288 To investigate the influence of the number of samples  $N_{\text{IS},1}$  and  $N_{\text{IS},2}$  on the CoV of  $\hat{P}_{F|\mathbf{d}}^{\text{IS}}$ ,  
 289 we consider two cases. In the first case, we take  $N_{\text{IS},1}$  and  $N_{\text{IS},2}$  equal to the number of  
 290 samples employed per level in the multi-level CE method, i.e.,  $N_{\text{IS},1} = N_{\text{IS},2} = N$ . In the  
 291 second case, we select the number of samples to ensure that  $\hat{\delta}_{\hat{P}_{F|\mathbf{d}}^{\text{IS}}}$  adheres to a target value  
 292  $\delta^*$ . For this, we vary  $N_{\text{IS},1}$  and  $N_{\text{IS},2}$  adaptively such that the sample estimates  $\hat{\delta}_1$  and  $\hat{\delta}_2$  are,  
 293 respectively, equal to target values  $\delta_1^*$  and  $\delta_2^*$  with  $\delta_1^* + \delta_2^* = \delta^*$ . A choice of  $\delta_1^* = \delta_2^* = \delta^*/\sqrt{2}$   
 294 is employed in the present study which ensures that  $\delta_{\hat{P}_{F|\mathbf{d}}^{\text{IS}}} \lesssim \delta^*$ .

#### 295 4.4. Separation of uncertainty

296 In many problems, the data contains information on only a sub-group of the random  
 297 variables appearing in the limit state function. For example,  $\boldsymbol{\Theta}$  can contain uncertain future  
 298 forcing variables, which cannot be learned. Let  $\boldsymbol{\Theta}_A$  denote the group of random variables  
 299 in  $\boldsymbol{\Theta}$  that cannot be learned and  $\boldsymbol{\Theta}_B$  denote the remaining random variables. In principle,  
 300 one can consider the likelihood function to be simply constant with respect to all random  
 301 variables in  $\boldsymbol{\Theta}_A$ . The methods described in the preceding sections then remain applicable,  
 302 and the posterior probability of failure can be estimated based on Eq. (22). However, in  
 303 certain applications it is convenient to evaluate the probability of failure conditional on  
 304 specific instances of  $\boldsymbol{\Theta}_B$  separately, using analytical or simulation-based methods [16, 11,  
 305 14]. In such cases, it is advantageous to express the posterior probability of failure in an  
 306 alternative form. Let  $p_{\boldsymbol{\Theta}}(\boldsymbol{\theta}) = p_{\boldsymbol{\Theta}_A|\boldsymbol{\Theta}_B}(\boldsymbol{\theta}_A|\boldsymbol{\theta}_B)p_{\boldsymbol{\Theta}_B|\mathbf{d}}(\boldsymbol{\theta}_B)$  be the prior PDF of  $\boldsymbol{\Theta}$ . The  
 307 posterior PDF of  $\boldsymbol{\Theta}$  is then given by  $p_{\boldsymbol{\Theta}|\mathbf{d}}(\boldsymbol{\theta}) = p_{\boldsymbol{\Theta}_A|\boldsymbol{\Theta}_B}(\boldsymbol{\theta}_A|\boldsymbol{\theta}_B)p_{\boldsymbol{\Theta}_B|\mathbf{d}}(\boldsymbol{\theta}_B)$ , where  $p_{\boldsymbol{\Theta}_B|\mathbf{d}}(\boldsymbol{\theta}_B)$   
 308 is the posterior PDF of  $\boldsymbol{\Theta}_B$  defined in analogy to Eq. (2). One can write the posterior  
 309 probability of failure in terms of  $\boldsymbol{\Theta}_A$  and  $\boldsymbol{\Theta}_B$  as

$$P_{F|\mathbf{d}} = \int_{\boldsymbol{\theta}_B \in \mathbb{R}^{n_{\boldsymbol{\theta}_B}}} P_{F|\boldsymbol{\Theta}_B}(\boldsymbol{\theta}_B) p_{\boldsymbol{\Theta}_B|\mathbf{d}}(\boldsymbol{\theta}_B) d\boldsymbol{\theta}_B, \quad (31)$$

310 where the conditional failure probability  $P_{F|\boldsymbol{\Theta}_B}(\boldsymbol{\theta}_B)$  is given by

$$P_{F|\boldsymbol{\Theta}_B}(\boldsymbol{\theta}_B) = \int_{\boldsymbol{\theta}_A \in \mathbb{R}^{n_{\boldsymbol{\theta}_A}}} I_F(\boldsymbol{\theta}_A, \boldsymbol{\theta}_B) p_{\boldsymbol{\Theta}_A|\boldsymbol{\Theta}_B}(\boldsymbol{\theta}_A|\boldsymbol{\theta}_B) d\boldsymbol{\theta}_A. \quad (32)$$

311 In Eqs. (31) and (32),  $n_{\boldsymbol{\theta}_A}$  and  $n_{\boldsymbol{\theta}_B}$  denote the dimension of  $\boldsymbol{\Theta}_A$  and  $\boldsymbol{\Theta}_B$ , respectively.  
 312 The formulation in the above equations offers two advantages. Firstly, the CE optimization  
 313 problem for updating model parameters  $\boldsymbol{\Theta}_B$ , that leads to the approximation of the posterior  
 314 PDF  $p_{\boldsymbol{\Theta}_B|\mathbf{d}}(\boldsymbol{\theta}_B)$ , is now solved in a lower-dimensional space. This reduces the computational  
 315 cost required for optimization and can help to address the degeneracy of the importance  
 316 sampling weights in high dimensions. Secondly, it enables one to evaluate  $P_{F|\boldsymbol{\Theta}_B}(\boldsymbol{\theta}_B)$  by  
 317 tailor-made approaches specific to the application at hand, thereby reducing the uncertainty

318 of the posterior failure probability estimator. The posterior probability of failure is then  
 319 estimated by evaluating the expectation of  $P_{F|\Theta_B}(\boldsymbol{\theta}_B)$  with respect to  $p_{\Theta_B|\mathbf{d}}(\boldsymbol{\theta}_B)$ . The  
 320 parametric density  $q_{\Theta_B}(\boldsymbol{\theta}_B; \hat{\boldsymbol{\nu}}_{L_1})$  for approximating  $p_{\Theta_B|\mathbf{d}}(\boldsymbol{\theta}_B)$  and estimating the marginal  
 321 likelihood can be constructed by the CE method through the procedure described in Section  
 322 3. However, the challenge lies in constructing an IS density associated with  $p_{\Theta_B|\mathbf{d}}(\boldsymbol{\theta}_B)$  to  
 323 efficiently perform the reliability integration, i.e., the expectation of  $P_{F|\Theta_B}(\boldsymbol{\theta}_B)$ , for which  
 324 the procedure in Section 4.1 cannot be directly applied.

325 The optimal IS density for evaluating the integral in Eq. (31) is given by

$$q_{P_{F|\mathbf{d}}}^*(\boldsymbol{\theta}_B) = \frac{1}{P_{F|\mathbf{d}}} P_{F|\Theta_B}(\boldsymbol{\theta}_B) p_{\Theta_B|\mathbf{d}}(\boldsymbol{\theta}_B). \quad (33)$$

326 Note that this optimal density is different from the one in Eq. (14). Hence, to determine  
 327 an approximation of the above density by the multi-level CE method, one needs to consider  
 328 an alternative distribution sequence that defines a smooth transition from  $p_{\Theta_B|\mathbf{d}}(\boldsymbol{\theta}_B)$ , or its  
 329 approximation  $q_{\Theta_B}(\boldsymbol{\theta}_B; \hat{\boldsymbol{\nu}}_{L_1})$ , to  $q_{P_{F|\mathbf{d}}}^*(\boldsymbol{\theta}_B)$  in Eq. (33). Such a distribution sequence can be  
 330 constructed by tempering the conditional probability function [24]:

$$h_2^k(\boldsymbol{\theta}_B) = \frac{1}{C_k} P_{F|\Theta_B}(\boldsymbol{\theta}_B)^{\alpha_k} p_{\Theta_B|\mathbf{d}}(\boldsymbol{\theta}_B), \quad (34)$$

331 where  $\{\alpha_k, k = 0, \dots, L_2\}$  are the tempering parameters satisfying  $0 = \alpha_0 < \alpha_1 < \dots <$   
 332  $\alpha_{L_2} = 1$  and  $C_k$  is the normalizing constant of  $h_2^k(\boldsymbol{\theta}_B)$ . The parametric IS density  $q_{\Theta_B}(\boldsymbol{\theta}_B; \hat{\boldsymbol{\nu}}_{L_2+L_1})$   
 333 is determined by approximating the above distribution sequence in a step-wise manner. The  
 334 associated CE optimization problems are solved sequentially, following similar steps as in  
 335 Section 3. An IS estimator of the posterior probability of failure is obtained as

$$\hat{P}_{F|\mathbf{d}}^{IS} = \frac{\frac{1}{N_{IS,2}} \sum_{i=1}^{N_{IS,2}} \hat{P}_{F|\Theta_B}(\boldsymbol{\theta}_B^{(2,i)}) W_{2,B}(\boldsymbol{\theta}_B^{(2,i)})}{\frac{1}{N_{IS,1}} \sum_{i=1}^{N_{IS,1}} L(\boldsymbol{\theta}_B^{(1,i)}|\mathbf{d}) W_{1,B}(\boldsymbol{\theta}_B^{(1,i)})}, \quad (35)$$

336 where  $W_{1,B}(\boldsymbol{\theta}_B) = \frac{p_{\Theta_B}(\boldsymbol{\theta}_B)}{q_{\Theta_B}(\boldsymbol{\theta}_B; \hat{\boldsymbol{\nu}}_{L_1})}$  and  $W_{2,B}(\boldsymbol{\theta}_B) = \frac{L(\boldsymbol{\theta}_B|\mathbf{d})p_{\Theta_B}(\boldsymbol{\theta}_B)}{q_{\Theta_B}(\boldsymbol{\theta}_B; \hat{\boldsymbol{\nu}}_{L_2+L_1})}$  are IS weights,  $\{\boldsymbol{\theta}_B^{(1,i)}, i = 1, \dots, N_{IS,1}\}$   
 337 and  $\{\boldsymbol{\theta}_B^{(2,i)}, i = 1, \dots, N_{IS,2}\}$  are independent samples generated from the IS densities  $q_{\Theta_B}(\boldsymbol{\theta}_B; \hat{\boldsymbol{\nu}}_{L_1})$   
 338 and  $q_{\Theta_B}(\boldsymbol{\theta}_B; \hat{\boldsymbol{\nu}}_{L_2+L_1})$ , respectively, and  $\hat{P}_{F|\Theta_B}(\boldsymbol{\theta}_B^{(2,i)})$  is the estimate of the conditional prob-  
 339 ability for sample  $\boldsymbol{\theta}_B^{(2,i)}$ . In the following, we discuss the evaluation of  $\hat{P}_{F|\Theta_B}(\boldsymbol{\theta}_B)$  for a special  
 340 case.

#### 341 4.4.1. Updating the first-passage failure probability of uncertain linear systems

342 A prominent example where the above formulation is useful is the estimation of first-  
 343 passage probability of systems subjected to random dynamic loads. In this context,  $F$   
 344 denotes the first-passage failure event,  $\Theta_A$  denotes the random variables characterizing the

345 future random excitation and  $\Theta_B$  denotes uncertain system parameters. Typically,  $\Theta_A$   
 346 is high dimensional and is independent of  $\Theta_B$ . It is well-known that applying standard  
 347 importance sampling with parametric IS density in a high-dimensional random variable space  
 348 can lead to poor estimates [3, 26]. This is related to the degeneracy of the IS weights in high  
 349 dimensions. Hence, advanced Monte Carlo methods that are designed for high dimensions  
 350 [37, 38] are commonly applied to estimate the first-passage probability. Evaluating the  
 351 posterior probability of failure based on Eqs. (31) and (32) enables the integration of these  
 352 methods into the framework of cross entropy-based Bayesian analysis to update first-passage  
 353 probabilities of engineering systems under future excitation.

354 The conditional probability  $P_{F|\Theta_B}(\theta_B)$  denotes the first-passage failure probability of  
 355 the deterministic system corresponding to a specific outcome  $\theta_B$  of the system parameters.  
 356 If the random excitation is a Gaussian process,  $\Theta_A$  is comprised of independent standard  
 357 Gaussian random variables. The conditional first-passage probability  $P_{F|\Theta_B}(\theta_B)$  can be  
 358 estimated by importance sampling from the outcome space of  $\Theta_A$ . In [2], an efficient IS  
 359 density,  $q_{\Theta_A|\Theta_B=\theta_B}(\theta_A)$ , of  $\Theta_A$  is suggested for the particular case where the system is linear,  
 360 which is defined by a weighted sum of Gaussian PDFs truncated on the failure domain of the  
 361 deterministic system defined by  $\theta_B$ . Accordingly, the conditional first-passage probability  
 362 is expressed by the modified integral

$$P_{F|\Theta_B}(\theta_B) = \int_{\theta_A \in \mathbb{R}^{n_{\theta_A}}} I_F(\theta_A, \theta_B) W_{2,A}(\theta_A) q_{\Theta_A|\Theta_B=\theta_B}(\theta_A) d\theta_A, \quad (36)$$

363 where  $W_{2,A}(\theta_A) = \frac{p_{\Theta_A}(\theta_A)}{q_{\Theta_A|\Theta_B=\theta_B}(\theta_A)}$  is the IS weight. By employing a one-sample estimator of  
 364 the above integral, the IS estimator for evaluating the posterior first-passage failure proba-  
 365 bility is given by:

$$\hat{P}_{F|\mathbf{d}}^{IS} = \frac{\frac{1}{N_{IS,2}} \sum_{i=1}^{N_{IS,2}} I_F(\theta_A^{(2,i)}, \theta_B^{(2,i)}) W_{2,A}(\theta_A^{(2,i)}) W_{2,B}(\theta_B^{(2,i)})}{\frac{1}{N_{IS,1}} \sum_{i=1}^{N_{IS,1}} L(\theta_B^{(1,i)}|\mathbf{d}) W_{1,B}(\theta_B^{(1,i)})}, \quad (37)$$

366 where  $\theta_A^{(2,i)}$  denotes a sample of the random vector  $\Theta_A$  characterizing the Gaussian exci-  
 367 tation, generated from the IS density  $q_{\Theta_A|\Theta_B=\theta_B^{(2,i)}}(\theta_A)$  suggested in [2]. The IS density  
 368  $q_{\Theta_B}(\theta_B; \hat{\nu}_{L_2+L_1})$  is determined by applying the multi-level CE method on the distribution  
 369 sequence in Eq. (34). For first-passage problems of linear systems, one can construct  
 370  $q_{\Theta_B}(\theta_B; \hat{\nu}_{L_2+L_1})$  efficiently, based on the framework introduced in [24, 25]. Here, an analyt-  
 371 ical approximation of the conditional first-passage probability,  $P_{F|\Theta_B}(\theta_B)$ , deduced based  
 372 on Rice's formula, is employed to solve the CE optimization problem. The use of the an-  
 373 alytical approximation facilitates smooth convergence of the CE method and reduces the  
 374 optimization effort without compromising much on accuracy. The IS estimator of  $P_{F|\Theta_B}(\theta_B)$   
 375 is applied for evaluating the posterior failure probability according to Eq. (37).

376 **5. Choice of parametric density**

377 In the CE method, the parametric density  $q_{\Theta}(\boldsymbol{\theta}; \boldsymbol{\nu})$  is typically chosen such that it con-  
 378 tains the nominal density of the uncertain model parameters. In the context of the Bayesian  
 379 updating problem, the nominal density corresponds to the prior PDF  $p_{\Theta}(\boldsymbol{\theta})$ . Without loss  
 380 of generality, we assume that the prior distribution of the random vector  $\Theta = \{\Theta_1; \dots; \Theta_{n_{\theta}}\}$   
 381 representing the uncertain model parameters is the independent standard Gaussian distri-  
 382 bution. Then the prior PDF is given by  $p_{\Theta}(\boldsymbol{\theta}) = \prod_{j=1}^{n_{\theta}} p_{\Theta_j}(\theta_j)$ , where for every  $j$ ,  $p_{\Theta_j}(\theta_j)$  is  
 383 a one-dimensional standard Gaussian PDF for  $\Theta_j$ . When the model parameters are a-priori  
 384 non-Gaussian and dependent, they are generated from the standard Gaussian random vector  
 385  $\Theta$  by means of the Nataf transformation [12] or the Rosenblatt transformation [20].

386 The Gaussian distribution family is a standard choice of the parametric family in the CE  
 387 method [36, 27]. To allow for efficient representation of multi-modal posterior distributions,  
 388 we consider a multivariate Gaussian mixture (GM) model as the parametric density. The  
 389 PDF of a GM model is defined as the sum of a number of Gaussian PDFs, each of them  
 390 multiplied by a weighing factor:

$$q_{\Theta}(\boldsymbol{\theta}; \boldsymbol{\nu}) = \sum_{s=1}^{n_{GM}} \pi_s f_G(\boldsymbol{\theta}; \boldsymbol{\mu}_s, \boldsymbol{\Sigma}_s), \quad (38)$$

391 where  $f_G(\boldsymbol{\theta}; \boldsymbol{\mu}_s, \boldsymbol{\Sigma}_s)$  is the  $s$ -th variate Gaussian PDF with mean  $\boldsymbol{\mu}_s$  and covariance matrix  
 392  $\boldsymbol{\Sigma}_s$  and  $\{\pi_s; s = 1, \dots, n_{GM}\}$  are normalized weights satisfying the condition  $\sum_{s=1}^{n_{GM}} \pi_s = 1$ .  
 393 In Eq. (38),  $n_{GM}$  denotes the number of modes, which can be fixed a-priori or selected on  
 394 the fly [17]. The parameter vector is given by  $\boldsymbol{\nu} = \{\pi_s, \boldsymbol{\mu}_s, \boldsymbol{\Sigma}_s; s = 1, \dots, n_{GM}\}$ , where  $\pi_s$   
 395 is scalar-valued,  $\boldsymbol{\mu}_s$  is a vector of dimension  $n_{\theta}$  and  $\boldsymbol{\Sigma}_s$  is an  $n_{\theta} \times n_{\theta}$  symmetric matrix.  
 396 This results in a total of  $n_{GM} \frac{n_{\theta}(n_{\theta}+3)}{2} + (n_{GM} - 1)$  unknown parameters in the parametric  
 397 density. For the uni-modal case, i.e.,  $n_{GM} = 1$ , closed form analytical expressions for the  
 398 parameter update in Eqs. (12) and (18) are available [36]. For the general case of  $n_{GM} > 1$ ,  
 399 the parameters are updated by means of an expectation-maximization (EM) algorithm. The  
 400 EM procedure and the updating rules for the parameters of the GM model are described in  
 401 [17] and are not further discussed here.

402 It is noted that in high dimensional problems, i.e., in problems where the number  $n_{\theta}$   
 403 of uncertain model parameters is large, the CE method with Gaussian densities performs  
 404 poorly. This is due to two reasons: the first is the degeneracy of the importance sampling  
 405 weight in high dimensions [3, 26]. The second reason is the number of parameters in the GM  
 406 model, which increases quadratically with  $n_{\theta}$ . This results in a rapid increase in the number  
 407 of samples per level  $N$  required to obtain an adequate estimate of the optimal parameter  
 408 values. In such cases, it is beneficial to consider alternative parametric densities, such as  
 409 the von-Mises-Fisher-Nakagami distribution family [43, 35], within the CE method.

410 **6. Numerical illustrations**

411 We investigate the performance of the proposed CE-based reliability updating (CEIS-  
 412 RelUp) method by means of three numerical examples. The first example considers the

413 reliability of a structural component subjected to fatigue updated with measurements of the  
414 crack size. Here we update the reliability of an infinite size plate with fatigue crack based on  
415 measurements of the crack size. The second example considers a geotechnical engineering  
416 problem. Here we apply CEIS-RelUp to update the reliability of an infinite clay slope based  
417 on measurements of the undrained shear strength. The third example involves dynamic  
418 reliability updating, where the first-passage probability of a randomly excited two-story  
419 moment-resisting frame is updated based on modal data.

420 The performance of the CEIS-RelUp method is assessed in terms of the sample mean and  
421 sample CoV of the estimates of  $P_{F|\mathbf{d}}$ , denoted by  $\hat{P}_{F|\mathbf{d}}$  and  $\hat{\delta}$  in this section, and in terms of  
422 the required computational effort. The sampling variance of the estimators  $\hat{P}_1$  and  $\hat{P}_2$  in the  
423 denominator and numerator of Eq. (22) contribute to the variability of  $\hat{P}_{F|\mathbf{d}}$ . The sample  
424 CoV of  $\hat{P}_1$  and  $\hat{P}_2$ , denoted by  $\hat{\delta}_1$  and  $\hat{\delta}_2$ , as well as the estimates of the marginal likelihood,  
425 denoted by  $\hat{c}_E$ , are also reported. The computational effort is assessed in terms of the  
426 number of samples of  $\Theta$  expended for CE optimization and reliability estimation.  $N_{CE,1}$  and  
427  $N_{CE,2}$ , respectively, denote the CE optimization effort required to construct the parametric  
428 IS densities  $q_{\Theta}(\theta; \hat{\nu}_{L_1})$  and  $q_{\Theta}(\theta; \hat{\nu}_{L_2+L_1})$ .  $N_{IS,1}$  and  $N_{IS,2}$ , respectively, denote the number  
429 of samples employed in the IS estimators  $\hat{P}_1$  and  $\hat{P}_2$  during reliability estimation. The sample  
430 size in the reliability estimation step is selected using two approaches. In the first approach,  
431 the sample size is taken equal to the number of samples per level for CE optimization, i.e.,  
432  $N_{IS,1} = N_{IS,2} = N$ . In the second approach,  $N_{IS,1}$  and  $N_{IS,2}$  are selected adaptively on the  
433 fly to ensure that an estimate of the CoV of the IS estimate of  $P_{F|\mathbf{d}}$  adheres to a specified  
434 target value  $\delta^*$ . The adaptive variant of the IS estimator is implemented according to the  
435 procedure described in [24]. The performance measures are averaged over 500 independent  
436 simulation runs in Examples 6.1 and 6.2 and 50 simulation runs in Example 6.3.

### 437 6.1. Fatigue crack growth

438 We consider an infinite size plate with fatigue crack, adapted from [13, 39]. The objective  
439 is to update the reliability of the plate based on measurements of the crack size. The rate  
440 of crack growth is described by Paris' Law as

$$\frac{da(n)}{dn} = C[\Delta S \sqrt{\pi a(n)}]^m, \quad (39)$$

441 where  $a$  is the size of the crack,  $n$  is the number of stress cycles,  $\Delta S$  is the stress range  
442 per cycle (constant stress amplitude is assumed) and  $C$  and  $m$  are empirically determined  
443 model parameters. The crack size as a function of the number of stress cycles  $n$  is given by  
444 [13]:

$$a(n) = \left[ \left(1 - \frac{m}{2}\right) C \Delta S^m \pi^{\frac{m}{2}} n + a_0^{1-\frac{m}{2}} \right]^{\frac{1}{1-\frac{m}{2}}}, \quad (40)$$

445 where  $a_0$  denotes the initial crack size. The failure event is defined in terms of the number  
446 of stress cycles to failure. The performance function is given by

$$g = n_c - n_f, \quad (41)$$

447 where  $n_c$  denotes the number of stress cycles required to reach a critical crack size of  $a_c$  and  
 448  $n_f$  denotes the number of stress cycles at which the reliability is estimated. For an infinite  
 449 plate,  $n_c$  is given by

$$\begin{aligned} n_c &= \frac{2}{(m-2)C(\sqrt{\pi}\Delta S)^m} \left[ \frac{1}{a_0^{\frac{m-2}{2}}} - \frac{1}{a_c^{\frac{m-2}{2}}} \right], m \neq 2 \\ &= \frac{1}{\pi C \Delta S^2} \ln \left( \frac{a_c}{a_0} \right), m = 2. \end{aligned} \quad (42)$$

450 The prior probabilistic description of the uncertain model parameters is given in Table 1.

Table 1: Prior probabilistic description of the parameters of the crack growth problem in Example 6.1.

Parameter	Distribution	Mean	Standard deviation	Correlation
$a_0$ [mm]	Exponential	1	1	-
$a_c$ [mm]	Deterministic	50	-	-
$\Delta S$ [Nmm <sup>-2</sup> ]	Normal	60	10	-
$(\ln(C)$ [N], $m$ [mm])	Bi-Normal	(-33,3.5)	(0.47,0.3)	$\rho_{\ln(C),m} = -0.9$

451 We estimate the reliability at  $n_f = 8 \times 10^5$  stress cycles. The prior value of the probability  
 452 of failure, based on  $2 \times 10^5$  standard Monte Carlo samples, is  $9.2 \times 10^{-3}$ . The failure  
 453 probability is updated via the likelihood function

$$L(\boldsymbol{\theta}|\mathbf{d}) = \prod_{i=1}^{n_M} \exp \left( -\frac{1}{2} \left( \frac{a(\boldsymbol{\theta}, n_i) - a_{m,i}}{\sigma_n} \right)^2 \right), \quad (43)$$

454 where  $n_M$  is the number of measurements,  $\sigma_n$  is the standard deviation of the measurement  
 455 noise,  $n_i$  is the number of stress cycles up to the  $i$ -th measurement and  $a_{m,i}$  are the crack  
 456 size measurements. We implement CEIS-RelUp with a uni-modal Gaussian distribution  
 457 as the parametric family. In the present example, where the number of uncertain model  
 458 parameters is  $n_\theta = 4$ , the Gaussian density is comprised of 14 unknown parameters, which  
 459 are updated analytically during CE optimization. We investigate the influence of the number  
 460 of measurements and the standard deviation of the measurement noise on the performance  
 461 of the method. The results for the two case studies are summarized in the following.

#### 462 6.1.1. Case study: Effect of standard deviation of measurement noise

463 We consider two measurements of crack size:

$$\begin{aligned} a_{m,1} &= 1.7\text{mm at } n_1 = 10^5 \text{ stress cycles} \\ a_{m,2} &= 1.8\text{mm at } n_2 = 3 \times 10^5 \text{ stress cycles} \end{aligned} \quad (44)$$

464 The posterior probability of failure,  $P_{F|\mathbf{d}}$ , is estimated with  $\sigma_n = 0.5\text{mm}$ ,  $0.25\text{mm}$  and  
 465  $0.125\text{mm}$ . In our experiment, the sample size, per level, for CE optimization is varied

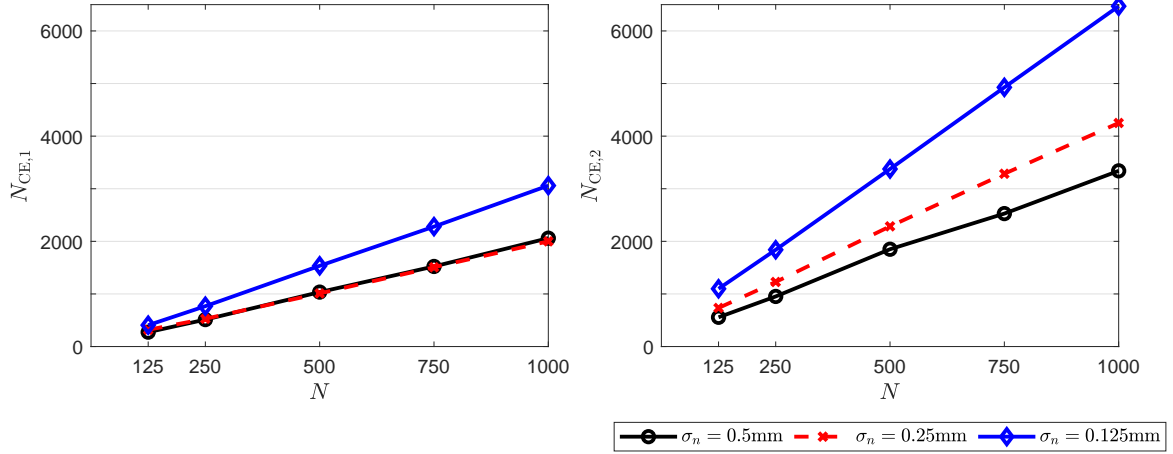


Figure 1: Cross entropy optimization effort for infinite size plate with fatigue crack

466 between  $N = 125$  and  $N = 1000$ . Fig. 1 shows the total number of samples, or equivalently  
 467 the number of model evaluations, required to construct the IS densities  $q_{\Theta}(\theta; \hat{\nu}_{L_1})$  and  
 468  $q_{\Theta}(\theta; \hat{\nu}_{L_2+L_1})$ . It is observed that the computational effort required for CE optimization  
 469 increases with decrease in  $\sigma_n$ . With decreasing standard deviation of the measurement noise,  
 470 the likelihood function gets more concentrated; consequently the target densities  $q_{P_{F|d}}^*(\theta)$   
 471 and  $p_{\Theta|d}(\theta)$  have lower standard deviation and their difference to the prior increases. This  
 472 results in an increase in the number of levels, and hence the number of samples, required  
 473 to reach the target densities by the multi-level CE method. Furthermore, we observe that  
 474  $N_{CE,2}$  is larger than  $N_{CE,1}$ , which indicates that the number of levels required by the CE  
 475 method to converge to  $q_{\Theta}(\theta; \hat{\nu}_{L_2+L_1})$  is more than that required for  $q_{\Theta}(\theta; \hat{\nu}_{L_1})$ . For the  
 476 values of  $\sigma_n$  considered, the number of levels range, on average, from  $L_1 = 2$  to 3 and  $L_2 =$   
 477 3 to 9 for the target densities  $p_{\Theta|d}(\theta)$  and  $q_{P_{F|d}}^*(\theta)$ , respectively. The required number of  
 478 levels indicates that the posterior is closer to the prior as compared to the optimal IS density  
 479 of the failure domain and the posterior.

480 We estimate the posterior failure probability with the non-adaptive ( $N_{IS}$ -NonAdap) and  
 481 adaptive ( $N_{IS}$ -Adap) variants of the IS estimator,  $\hat{P}_{F|d}$ . In the latter case, the target CoV  
 482 of  $\hat{P}_{F|d}$  is set to  $\delta^* = 0.10$  and 0.05. Recall that the contribution to the CoV of  $\hat{P}_{F|d}$  comes  
 483 from the two IS estimators,  $\hat{P}_1$  and  $\hat{P}_2$ , in the denominator and numerator of Eq. (22).  
 484 In the adaptive case, the sample sizes of these estimators, i.e.,  $N_{IS,1}$  and  $N_{IS,2}$ , are selected  
 485 adaptively such that the respective sample CoVs adhere to the target values  $\delta_1^*$  and  $\delta_2^*$ , where  
 486  $\delta_1^* = \delta_2^* = \delta^*/\sqrt{2}$ . These target CoVs are equal to 0.071 for  $\delta^* = 0.10$  and 0.035 for  $\delta^* = 0.05$ .  
 487 The Monte Carlo estimate of the failure probability, using  $2 \times 10^5$  samples obtained from  
 488 the posterior PDF through rejection sampling, is  $3.7 \times 10^{-3}$  (CoV  $\approx 3.7\%$ ),  $1.7 \times 10^{-3}$  (CoV  
 489  $\approx 5.4\%$ ) and  $9.5 \times 10^{-5}$  (CoV  $\approx 23\%$ ) for  $\sigma_n = 0.5\text{mm}$ ,  $0.25\text{mm}$  and  $0.125\text{mm}$ , respectively.  
 490 The simulation results for  $N = 250$  and 500 are reported in Table 2. The sample mean of the

491 posterior failure probability estimates are comparable with the reference solution, for all  $\sigma_n$ .  
492 However, the sampling variability of  $\hat{P}_{F|\mathbf{d}}$  changes significantly with  $\sigma_n$ . As  $\sigma_n$  decreases, the  
493 posterior PDF becomes significantly different from the prior, and the failure event under the  
494 posterior probability measure becomes increasingly rare. These factors increase the number  
495 of levels for convergence due to the reduced ability of the parametric family in describing  
496 the target densities  $q_{P_{F|\mathbf{d}}}^*(\boldsymbol{\theta})$  and  $p_{\Theta|\mathbf{d}}(\boldsymbol{\theta})$ , thereby leading to an increase in the sample CoV  
497 of the IS estimators for small  $\sigma_n$ . Hence, when the sample size of these estimators is fixed,  
498 i.e., for the non-adaptive case with  $N_{\text{IS},1} = N_{\text{IS},2} = N$ , we observe a monotonic increase in  
499 the respective sample CoVs, i.e.,  $\hat{\delta}_1$  and  $\hat{\delta}_2$  in Table 2, with decrease in  $\sigma_n$ . The increase is  
500 significant for  $\hat{\delta}_2$ . Accordingly, when the sample size is selected adaptively, the IS estimators  
501 require a larger number of samples to achieve the target CoV for small values of  $\sigma_n$ .

Table 2: Posterior failure probability estimates for fatigue crack growth, with two measurements, for different standard deviation of measurement noise. Reference value of the probability of failure, based on  $2 \times 10^5$  samples obtained through rejection sampling, is  $3.7 \times 10^{-3}$ ,  $1.7 \times 10^{-3}$  and  $9.5 \times 10^{-5}$  for  $\sigma_n = 0.5\text{mm}$ ,  $0.25\text{mm}$  and  $0.125\text{mm}$ , respectively.

			$\hat{c}_E$	$\hat{P}_{F \mathbf{d}}$	$\hat{\delta}$	$\hat{\delta}_1$	$\hat{\delta}_2$	$N_{\text{IS},1}$	$N_{\text{IS},2}$	$N_{\text{T}}$
$\sigma_n = 0.500$	$N = 250$	$N_{\text{IS-NonAdap}}$	0.159	$3.86 \times 10^{-3}$	0.09	0.03	0.10	250	250	1965
		$N_{\text{IS-Adap}} (\delta^* = 0.10)$	0.159	$3.85 \times 10^{-3}$	0.11	0.07	0.08	28	432	1926
		$N_{\text{IS-Adap}} (\delta^* = 0.05)$	0.159	$3.82 \times 10^{-3}$	0.07	0.04	0.06	120	1150	2735
	$N = 500$	$N_{\text{IS-NonAdap}}$	0.161	$3.84 \times 10^{-3}$	0.08	0.01	0.07	500	500	3885
		$N_{\text{IS-Adap}} (\delta^* = 0.10)$	0.159	$3.87 \times 10^{-3}$	0.08	0.06	0.06	19	568	3472
		$N_{\text{IS-Adap}} (\delta^* = 0.05)$	0.160	$3.83 \times 10^{-3}$	0.06	0.04	0.05	71	989	3945
$\sigma_n = 0.250$	$N = 250$	$N_{\text{IS-NonAdap}}$	0.076	$1.65 \times 10^{-3}$	0.21	0.05	0.20	250	250	2255
		$N_{\text{IS-Adap}} (\delta^* = 0.10)$	0.074	$1.65 \times 10^{-3}$	0.12	0.08	0.09	48	564	2367
		$N_{\text{IS-Adap}} (\delta^* = 0.05)$	0.074	$1.64 \times 10^{-3}$	0.07	0.04	0.06	195	1473	3423
	$N = 500$	$N_{\text{IS-NonAdap}}$	0.075	$1.64 \times 10^{-3}$	0.07	0.02	0.07	500	500	4295
		$N_{\text{IS-Adap}} (\delta^* = 0.10)$	0.074	$1.66 \times 10^{-3}$	0.10	0.07	0.07	26	608	3929
		$N_{\text{IS-Adap}} (\delta^* = 0.05)$	0.075	$1.65 \times 10^{-3}$	0.06	0.04	0.05	104	1220	4619
$\sigma_n = 0.125$	$N = 250$	$N_{\text{IS-NonAdap}}$	0.034	$9.75 \times 10^{-5}$	0.30	0.05	0.30	250	250	3108
		$N_{\text{IS-Adap}} (\delta^* = 0.10)$	0.034	$9.54 \times 10^{-5}$	0.12	0.06	0.10	61	868	3536
		$N_{\text{IS-Adap}} (\delta^* = 0.05)$	0.034	$9.54 \times 10^{-5}$	0.09	0.04	0.08	274	2609	5490
	$N = 500$	$N_{\text{IS-NonAdap}}$	0.034	$9.68 \times 10^{-5}$	0.26	0.02	0.26	500	500	5910
		$N_{\text{IS-Adap}} (\delta^* = 0.10)$	0.034	$9.63 \times 10^{-5}$	0.10	0.06	0.08	45	723	5678
		$N_{\text{IS-Adap}} (\delta^* = 0.05)$	0.034	$9.67 \times 10^{-5}$	0.07	0.04	0.06	157	2032	7099

502 The performance of CEIS-RelUp is assessed for different sample size  $N$  during CE opti-  
503 mization. We observe that the sample mean of the posterior failure probability estimates is  
504 broadly similar for all  $N$ . However, there is significant change in the sampling variability of  
505 the estimators and the required computational effort. The variation in the sample CoV of  
506  $\hat{P}_{F|\mathbf{d}}$  and the total computational effort, for  $\sigma_n = 0.5\text{mm}$  and  $0.125\text{mm}$ ,  $\delta^* = 0.10$  and  $0.05$ ,  
507 are shown in Fig. 2. For the non-adaptive variant of the IS estimator,  $N_{\text{IS-NonAdap}}$ , an  
508 increase in  $N$  reduces the sample CoV,  $\hat{\delta}$ , of the posterior failure probability estimator. This

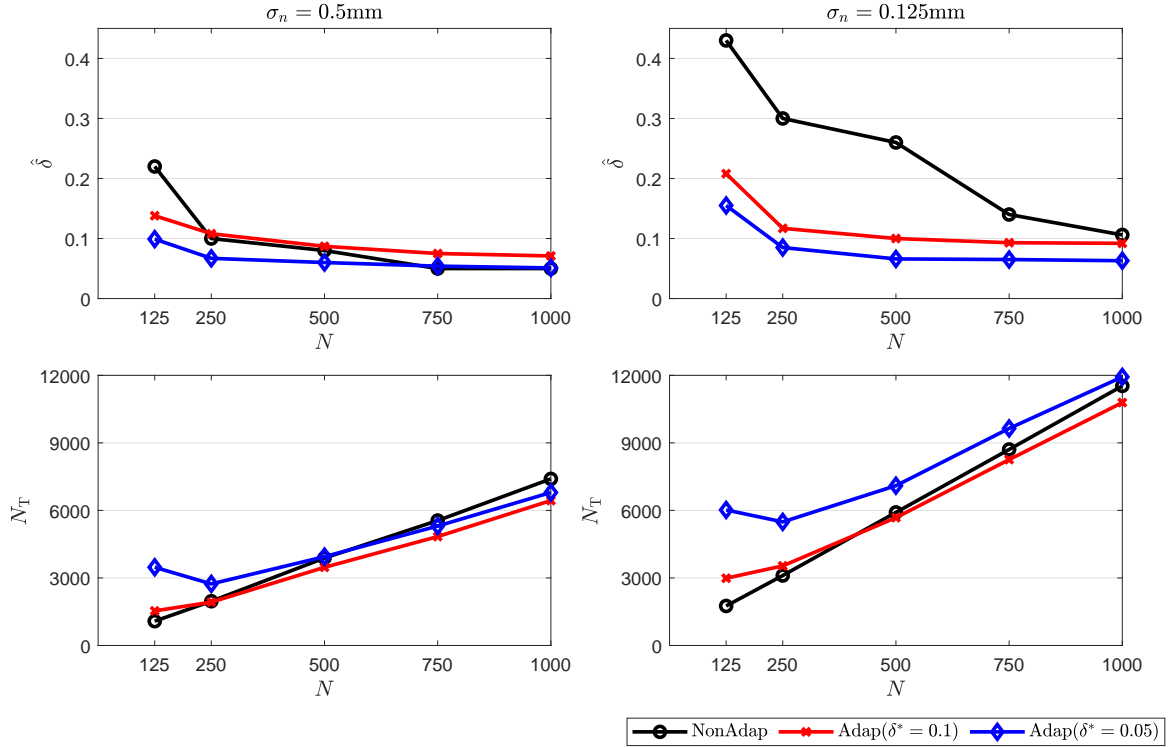


Figure 2: Coefficient of variation of posterior failure probability estimates and total computational effort for infinite size plate with fatigue crack

509 behavior is due to two factors. First, the number of effective samples available to fit the  
510 parametric densities increases with  $N$ . This results in improved estimates of the parameter  
511 vectors  $\hat{\nu}_{L_1}$  and  $\hat{\nu}_{L_2+L_1}$ , and better approximation of the respective optimal IS densities.  
512 Second, an increase in  $N$  implies a monotonic increase in the sample size of the IS estima-  
513 tors  $\hat{P}_1$  and  $\hat{P}_2$ , which leads to a reduction in the sample CoVs  $\hat{\delta}_1$  and  $\hat{\delta}_2$ , respectively. The  
514 decrease in sampling fluctuations for  $N_{\text{IS-NonAdap}}$  is, however, at the expense of increased  
515 computational effort. In case of  $N_{\text{IS-Adap}}$ , the sample CoV  $\delta_1$  is close to the target value,  
516 i.e.,  $\delta_1^* = 0.071$  for  $\delta^* = 0.10$  and  $\delta_1^* = 0.035$  for  $\delta^* = 0.05$ , for all  $N$ . The estimates of  $\delta_2$  are  
517 initially large for  $\delta^* = 0.10$ , but they gradually reduce to 0.071 as  $N$  increases. For  $\delta^* = 0.05$ ,  
518 however,  $\hat{\delta}_2$  remains larger than the target value 0.035. This is due to inaccuracy in the esti-  
519 mator of  $\delta_2$ , in Eq. (30), used for the adaptive selection of  $N_{\text{IS},2}$ . The sub-optimality in the  
520 IS density  $q_{\Theta}(\theta; \hat{\nu}_{L_2+L_1})$  for small  $\sigma_n$  induces possible bias in the estimator, due to which it  
521 decays faster than the true value. We note that in the adaptive variant of the method, the  
522 number of samples for estimation of the denominator can be smaller than  $N$ , whereas for the  
523 numerator it is always greater than  $N$ . This is because checking the termination criterion  
524 for the numerator requires  $N$  samples from the final density [35]. Overall, it is observed  
525 that the performance of  $N_{\text{IS-NonAdap}}$  and  $N_{\text{IS-Adap}}$  are comparable for  $\sigma_n = 0.5\text{mm}$ . For

526  $\sigma_n = 0.125\text{mm}$ , the adaptive variant of the IS estimator exhibits superior performance. In  
 527 the latter case,  $N_{\text{IS-NonAdap}}$  requires 11530 samples to yield a sample CoV of 10% of the IS  
 528 estimator  $\hat{P}_{F|\mathbf{d}}$ , whereas  $N_{\text{IS-Adap}}$  yields a sample CoV of 10% and 6% with approximately  
 529 5500 and 7000 samples, respectively.

### 530 6.1.2. Case study: Effect of number of measurements

531 To investigate the influence of the number of measurements,  $n_M$ , on the performance of  
 532 CEIS-RelUp, we consider two additional observations of the crack size:

$$\begin{aligned} a_{m,3} &= 1.9\text{mm at } n_3 = 4 \times 10^5 \text{ stress cycles} \\ a_{m,4} &= 2.1\text{mm at } n_4 = 5 \times 10^5 \text{ stress cycles} \end{aligned} \quad (45)$$

533 The posterior probability of failure,  $P_{F|\mathbf{d}}$ , for  $\sigma_n = 0.5\text{mm}$  is  $5.1 \times 10^{-4}$  (CoV  $\approx 10\%$ ). The  
 534 reference solution is evaluated based on  $2 \times 10^5$  samples obtained through rejection sampling.  
 535 We evaluate  $P_{F|\mathbf{d}}$  by CEIS-RelUp, using non-adaptive and adaptive selection of the sample  
 536 size of the IS estimator. The results with  $N_{\text{IS-Adap}}$  correspond to  $\delta^* = 0.10$ . We select  
 537  $N = 250$  and  $500$  samples per level during CE optimization. It is observed that the CE  
 538 optimization effort, i.e., the number of levels required to construct the IS densities  $q_{\Theta}(\boldsymbol{\theta}; \hat{\boldsymbol{\nu}}_{L_1})$   
 539 and  $q_{\Theta}(\boldsymbol{\theta}; \hat{\boldsymbol{\nu}}_{L_1+L_2})$ , increases with the number of measurements. The increase is marginal for  
 540  $q_{\Theta}(\boldsymbol{\theta}; \hat{\boldsymbol{\nu}}_{L_1})$ , but approximately twice for  $q_{\Theta}(\boldsymbol{\theta}; \hat{\boldsymbol{\nu}}_{L_1+L_2})$ . The results of reliability estimation  
 541 are reported in Table 3. The sample mean of the posterior failure probability estimator,  
 542  $\hat{P}_{F|\mathbf{d}}$ , compares well with the reference solution. For  $N_{\text{IS-NonAdap}}$ , the sample CoV,  $\hat{\delta}$ , of  
 543  $\hat{P}_{F|\mathbf{d}}$  decreases with increase in  $N$ , which was also observed in Table 2. For  $N_{\text{IS-Adap}}$ ,  $\hat{\delta}$   
 544 remains close to the specified target value. We observe that an increase in the number of  
 545 measurements causes a significant increase in the sample CoV of the IS estimators  $\hat{P}_1$  and  $\hat{P}_2$ ,  
 546 leading to larger sampling fluctuations in  $\hat{P}_{F|\mathbf{d}}$ . When the sample size of these estimators,  
 547 i.e.,  $N_{\text{IS},1}$  and  $N_{\text{IS},2}$ , are fixed to  $N$ , the respective sample CoVs  $\hat{\delta}_1$  and  $\hat{\delta}_2$  are approximately  
 548 twice of those obtained for  $n_M = 2$ . Similarly, when  $N_{\text{IS},1}$  and  $N_{\text{IS},2}$  are selected adaptively,  
 549 the number of samples required to meet the target CoV increases with  $n_M$ . Finally, we  
 550 observe that  $N_{\text{IS-Adap}}$  remains more efficient than  $N_{\text{IS-NonAdap}}$ , since it yields a smaller  
 551 sample CoV of  $\hat{P}_{F|\mathbf{d}}$  with comparable total computational effort.

Table 3: Posterior failure probability estimates for fatigue crack growth by CEIS-RelUp, with  $n_M = 4$  and  $\sigma_n = 0.5\text{mm}$ . Reference value of the probability of failure, based on  $2 \times 10^5$  samples obtained through rejection sampling, is  $5.1 \times 10^{-4}$ .

		$\hat{c}_E$	$\hat{P}_{F \mathbf{d}}$	$\hat{\delta}$	$\hat{\delta}_1$	$\hat{\delta}_2$	$N_{\text{IS},1}$	$N_{\text{IS},2}$	$N_T$
$N = 250$	$N_{\text{IS-NonAdap}}$	0.087	$5.38 \times 10^{-4}$	0.23	0.05	0.22	250	250	2582
	$N_{\text{IS-Adap}} (\delta^* = 0.10)$	0.085	$5.42 \times 10^{-4}$	0.12	0.08	0.09	57	617	2756
$N = 500$	$N_{\text{IS-NonAdap}}$	0.086	$5.41 \times 10^{-4}$	0.18	0.02	0.17	500	500	4918
	$N_{\text{IS-Adap}} (\delta^* = 0.10)$	0.085	$5.30 \times 10^{-4}$	0.10	0.07	0.08	37	773	4728

552 *6.2. Stability of an infinite clay slope*

553 In this example, we apply the CEIS-RelUp approach to update the reliability of a sat-  
 554 urated (infinite) clay slope under undrained conditions. The slope, shown in Fig. 3, has a  
 555 height of  $H = 5\text{m}$ , a slope angle of  $\beta = 15^\circ$  and a saturated unit weight of  $\gamma = 20\text{kN/m}^3$ .  
 556 The short-term shear strength of the clay is characterized by the undrained shear strength,  
 557 which is assumed to vary with depth from the soil surface. The factor of safety governing  
 558 the slope stability is given by [18]

$$FS(z) = \frac{s_u(z)}{\gamma z \sin \beta \cos \beta}, \quad (46)$$

559 where  $s_u(z)$  denotes the undrained shear strength at a depth  $z$  below the ground surface.

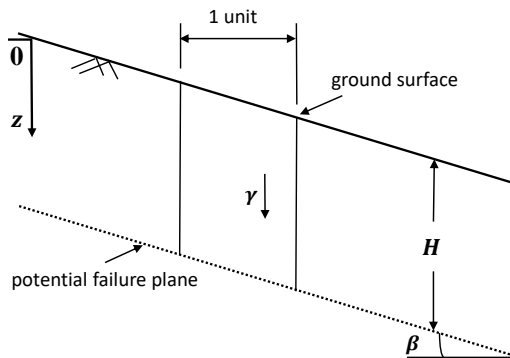


Figure 3: Infinite clay slope in Example 6.2

560 The failure event  $F$  of the slope is defined as  $FS_{\min}$  being  $< 1.0$ , where  $FS_{\min}$  is the  
 561 minimum factor of safety over the height of the slope. The depth dependent nature of the  
 562 undrained shear strength is characterized by the non-stationary random field model [22]

$$s_u(z) = s_{u0} + b\gamma z \exp[w(z)], \quad (47)$$

563 where  $s_{u0}$  is the undrained shear strength at the ground surface,  $b$  is a trend parameter that  
 564 determines the rate of increase of strength with soil depth and  $w(z)$  is the randomly fluctu-  
 565 ating component of  $s_u$ , which is modeled as a one-dimensional zero mean Gaussian random  
 566 field with constant standard deviation,  $\sigma_w = 0.24$ . To characterize the spatial correlation of  
 567  $s_u$ , we assume an exponential auto-correlation function of  $w(z)$ , with a correlation length of  
 568 1.9m [23].  $w(z)$  is numerically represented in terms of a finite number of random variables  
 569 through the Karhunen-Loève (KL) expansion:

$$w(z) = \sum_{i=1}^{n_{KL}} \sqrt{\lambda_i} \phi_i(z) \theta_i^{KL}, \quad (48)$$

570 where  $\{(\lambda_i, \phi_i(z)), i = 1, \dots, n_{KL}\}$  are eigenpairs of the auto-covariance function, arranged  
 571 in decreasing order of magnitude of the eigenvalues, and  $\{\theta_i^{KL}, i = 1, \dots, n_{KL}\}$  are indepen-  
 572 dent standard Gaussian random variables. We consider  $n_{KL} = 10$  eigenmodes in the KL  
 573 expansion. Following [23], we model the prior distribution of the parameters  $s_{u0}$  and  $b$  by  
 574 lognormal random variables, with means  $\mu_{s_{u0}} = 14.67\text{kPa}$  and  $\mu_b = 0.272$ , and standard  
 575 deviations  $\sigma_{s_{u0}} = 4.04\text{kPa}$  and  $\sigma_b = 0.189$ . In this way, a total of  $n_{\theta} = 12$  random variables  
 576 are required to represent the non-stationary random field  $s_u(z)$ .

577 For the purpose of reliability analysis, we discretize the soil profile into 100 equal slices  
 578 of height  $\Delta h = H/100$ . The factor of safety is evaluated at the base of each slice, resulting  
 579 in 100 different factors of safety  $\{FS(z_i), i = 1, \dots, 100\}$ , where  $z_i = i\Delta h$ . The minimum  
 580 factor of safety is evaluated as  $FS_{\min} = \min_{i=1, \dots, 100} FS(z_i)$ . Without measurements, the  
 581 prior probability of slope failure is  $1.49 \times 10^{-1}$  as obtained from  $10^5$  standard Monte Carlo  
 582 samples. The following measurements of the undrained shear strength are used to update  
 583 the failure probability:

$$\begin{aligned} s_{u_{m,1}} &= 17.8\text{kPa} \text{ at } z_{m,1} = 1.5\text{m} \\ s_{u_{m,2}} &= 24.5\text{kPa} \text{ at } z_{m,2} = 3.0\text{m} \\ s_{u_{m,3}} &= 30.5\text{kPa} \text{ at } z_{m,3} = 4.5\text{m} \end{aligned} \quad (49)$$

584 The measurement result  $s_{u_{m,i}}$  at a given location  $z_{m,i}$  is related to the true value by means of  
 585 independent multiplicative error  $\epsilon_{m,i}$ , that is assumed to follow a lognormal distribution with  
 586 median equal to one and constant standard deviation. With this assumption, the likelihood  
 587 function is given by [40]

$$L(\boldsymbol{\theta}|\mathbf{d}) = \exp\left(-\sum_{i=1}^{n_M} \frac{[\ln s_{u_{m,i}} - \ln s_u(z_{m,i}, \boldsymbol{\theta})]^2}{2\sigma_{\ln \epsilon_{m,i}}^2}\right), \quad (50)$$

588 where  $\sigma_{\ln \epsilon_{m,i}} = \sqrt{\ln(1 + \text{CoV}_{\epsilon_{m,i}}^2)}$  is the standard deviation of  $\ln \epsilon_{m,i}$ . The coefficient of  
 589 variation of  $\epsilon_{m,i}$  is set to  $\text{COV}_{\epsilon_{m,i}} = 5\%$  in this example. A reference value of the posterior  
 590 probability of failure based on  $10^6$  samples obtained through rejection sampling is  $6.37 \times$   
 591  $10^{-4}$  ( $\text{CoV} \approx 4\%$ ).

592 We implement CEIS-RelUp with a uni-modal Gaussian distribution as the parametric  
 593 family. In the present example, where the number of uncertain model parameters is  $n_{\theta} = 12$ ,  
 594 the Gaussian density is comprised of 90 unknown parameters. In Fig. 4 we show the prior  
 595 and posterior statistics of the undrained shear strength,  $s_u$ , and the factor of safety,  $FS$ .  
 596 The estimates of the prior statistics are obtained through standard Monte Carlo simulation  
 597 from the prior PDF. The estimates of the posterior statistics are obtained from CEIS-RelUp,  
 598 through importance sampling from the fitted IS densities  $q_{\boldsymbol{\theta}}(\boldsymbol{\theta}; \hat{\boldsymbol{\nu}}_{L_1})$  and  $q_{\boldsymbol{\theta}}(\boldsymbol{\theta}; \hat{\boldsymbol{\nu}}_{L_2+L_1})$ . A  
 599 comparison of the estimates from CEIS-RelUp with the ones obtained through rejection  
 600 sampling (RS) demonstrates good agreement. The mean of the posterior of  $s_u$  conditional  
 601 on the domain of the failure event,  $F$ , is close to the mean of the unconditional posterior,  
 602 which indicates that the PDF of the uncertain model parameters shifts towards the failure  
 603 domain after the updating. There is a reduction in the spread of the updated PDF, as

604 indicated by smaller standard deviation of the posterior of  $s_u$  in comparison to the prior,  
 605 which, in turn, results in a lower posterior probability of failure. The variation in the mean  
 606 of  $FS$  indicates that failure is more likely to occur.

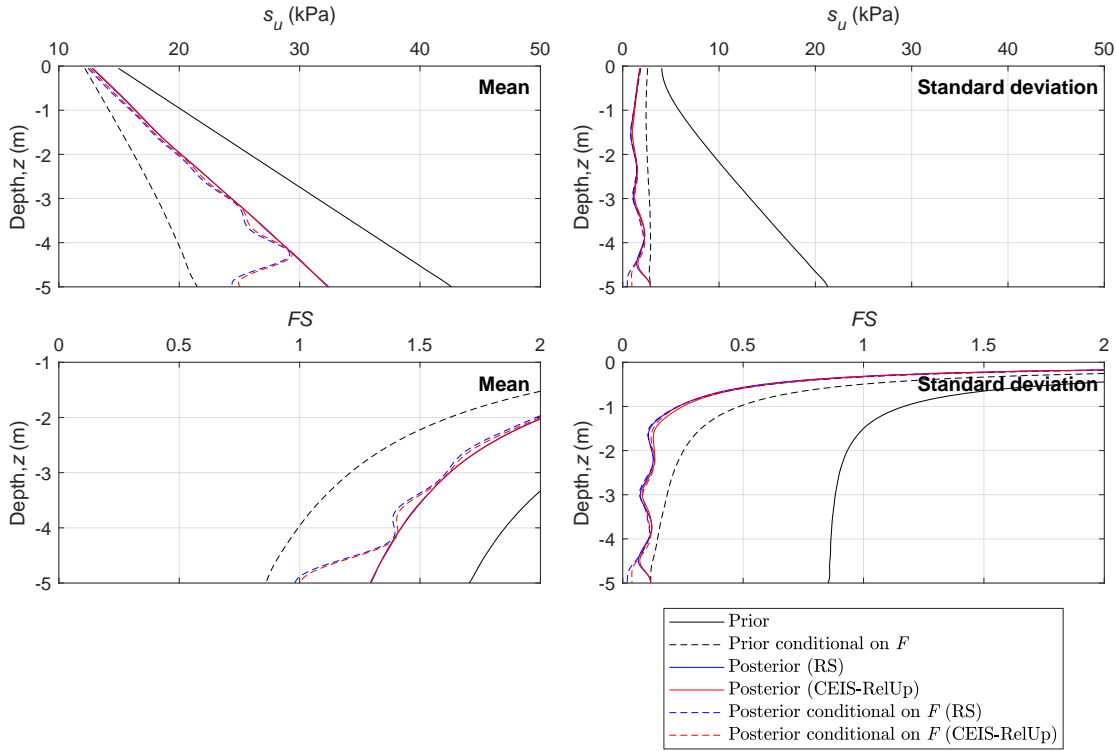


Figure 4: Prior and posterior statistics of the undrained shear strength,  $s_u$ , and the factor of safety,  $FS$ . Top-left: Variation of mean of  $s_u$  with depth. Top-right: Variation of standard deviation of  $s_u$  with depth. Bottom-left: Variation of mean of  $FS$  with depth. Bottom-right: Variation of standard deviation of  $FS$  with depth.

607 The results of reliability estimation, as well as the computational effort required to  
 608 construct the IS densities  $q_{\Theta}(\theta; \hat{\nu}_{L_1})$  and  $q_{\Theta}(\theta; \hat{\nu}_{L_2+L_1})$ , are reported in Table 4. We employ  
 609 the non-adaptive ( $N_{IS}$ -NonAdap) and adaptive ( $N_{IS}$ -Adap) variants of the IS estimator,  
 610  $\hat{P}_{F|d}$ , to estimate the posterior failure probability. In the latter case, the target CoV of  $\hat{P}_{F|d}$   
 611 is set to  $\delta^* = 0.10$ , which corresponds to target values  $\delta_1^* = \delta_2^* = 0.071$  of the CoV of the  
 612 estimators  $\hat{P}_1$  and  $\hat{P}_2$ , in the denominator and numerator of Eq. (22). The estimates of  $N_{CE,1}$   
 613 and  $N_{CE,2}$  indicate that the required CE optimization effort is higher in the second stage,  
 614 i.e., the number of levels required to construct  $q_{\Theta}(\theta; \hat{\nu}_{L_2+L_1})$  is approximately twice of that  
 615 required for  $q_{\Theta}(\theta; \hat{\nu}_{L_1})$ . As the sample size per level  $N$  increases, we observe a decrease in  
 616 the required number of levels for convergence of the CE method. This is due to an increase  
 617 in the number of effective samples available to fit the parametric densities, which facilitates  
 618 faster convergence of the CE method.

619 With  $N = 500$  samples per level, we observe an underestimation in the posterior failure  
620 probability estimates as obtained from CEIS-RelUp. This is due to bias in the estimates  
621 of the numerator  $\hat{P}_2$ . The estimate of the marginal likelihood, although not reported, is  
622 observed to be accurate for all  $N$ . In comparison, approximating the optimal IS density  
623 of the numerator, i.e.,  $q_{P_{F|d}}^*(\boldsymbol{\theta})$ , is more challenging. For a small  $N$ , the available number  
624 of effective samples is not sufficient to adequately approximate  $q_{P_{F|d}}^*(\boldsymbol{\theta})$ , leading to bias in  
625 the failure probability estimates. With increase in  $N$ , we also observe a reduction in the  
626 sampling variability of the IS estimators. With  $N_{\text{IS-NonAdap}}$ , there is a gradual decrease in  
627 the sample CoV of the IS estimators  $\hat{P}_1$  and  $\hat{P}_2$ , and hence of the estimator  $\hat{P}_{F|d}$ . The results  
628 with non-adaptive and adaptive variants of the IS estimator indicate that  $\hat{P}_2$  has a larger  
629 variability than  $\hat{P}_1$ , which indicates reduced flexibility of the parametric density in describing  
630 the posterior PDF over the failure domain. Overall, both variants of the IS estimator require  
631 similar total computational effort,  $N_T$ . Hence, selecting the sample size of the IS estimators  
632 adaptively does not offer a clear advantage in this example. This is because a large number  
633 of samples per level  $N$  is required to obtain an adequate parametric IS density for estimating  
634 the updated failure probability. Both variants of the method employ at least  $N$  samples for  
635 estimation and when  $N$  is large the CoV of the probability estimate is already small enough  
636 with  $N$  samples.

Table 4: Posterior failure probability estimates of infinite clay slope by CEIS-RelUp. Reference value of the posterior probability of failure based on  $10^6$  samples obtained through rejection sampling is  $6.37 \times 10^{-4}$ .

		$N_{\text{CE},1}$	$N_{\text{CE},2}$	$\hat{P}_{F d}$	$\hat{\delta}$	$\hat{\delta}_1$	$\hat{\delta}_2$	$N_{\text{IS},1}$	$N_{\text{IS},2}$	$N_T$
$N = 500$	$N_{\text{IS-NonAdap}}$	2275	5319	$5.71 \times 10^{-4}$	0.35	0.09	0.34	500	500	8594
	$N_{\text{IS-Adap}} (\delta^* = 0.10)$	2275	5319	$5.94 \times 10^{-4}$	0.18	0.07	0.17	437	3412	11443
$N = 750$	$N_{\text{IS-NonAdap}}$	2798	6250	$6.23 \times 10^{-4}$	0.15	0.09	0.14	750	750	10548
	$N_{\text{IS-Adap}} (\delta^* = 0.10)$	2798	6250	$6.30 \times 10^{-4}$	0.13	0.07	0.11	237	1911	11196
$N = 1000$	$N_{\text{IS-NonAdap}}$	3399	7282	$6.26 \times 10^{-4}$	0.11	0.05	0.10	1000	1000	12681
	$N_{\text{IS-Adap}} (\delta^* = 0.10)$	3399	7282	$6.38 \times 10^{-4}$	0.11	0.07	0.08	201	1694	12576
$N = 2000$	$N_{\text{IS-NonAdap}}$	6253	12898	$6.36 \times 10^{-4}$	0.08	0.03	0.07	2000	2000	23151
	$N_{\text{IS-Adap}} (\delta^* = 0.10)$	6253	12898	$6.39 \times 10^{-4}$	0.09	0.06	0.06	140	2364	21746

### 637 6.3. First-passage failure of a two-story moment-resisting frame

638 We apply CEIS-RelUp to update the first-passage failure probability of a two-story  
639 moment-resisting frame, earlier studied in [5], using its identified natural frequencies. A  
640 two degree-of-freedom shear building model, shown in Fig. 5, is used to model the structure  
641 in order to identify the inter-story stiffnesses and story masses, and to predict the reliability.  
642 The inter-story stiffnesses are parameterized as  $k_1 = \alpha_1 \bar{k}_1$  and  $k_2 = \alpha_2 \bar{k}_2$ , where  $\alpha_1$  and  $\alpha_2$   
643 are the stiffness parameters to be identified, and  $\bar{k}_1 = \bar{k}_2 = 29.7 \times 10^6 \text{N/m}$  are the nominal  
644 values for the inter-story stiffnesses of the first and second stories, respectively. The story  
645 masses are parameterized as  $m_1 = \alpha_3 \bar{m}_1$  and  $m_2 = \alpha_4 \bar{m}_2$ , where  $\alpha_3$  and  $\alpha_4$  are the mass  
646 parameters to be updated, and  $\bar{m}_1 = 16.5 \times 10^3 \text{kg}$  and  $\bar{m}_2 = 16.1 \times 10^3 \text{kg}$  are the nominal

647 values for the first- and second-story masses, respectively. The prior PDF for  $\alpha_1$  to  $\alpha_4$  is  
 648 given by the product of four lognormal PDFs with most probable values 1.3, 0.8, 0.95 and  
 649 0.95, and standard deviations 1, 1, 0.1 and 0.1, respectively.

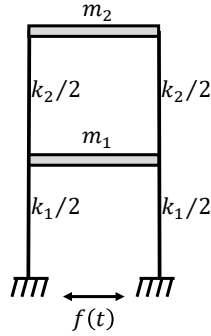


Figure 5: Two degree-of-freedom shear building model in Example 6.3

650 The first-passage failure probability of the structure subjected to a stochastic ground  
 651 excitation is predicted using the shear building model. The response of interest is the inter-  
 652 story drift between the first and the second stories. Failure is defined as the event that  
 653 the inter-story drift exceeds a threshold level of  $h^*$  within a duration of  $T = 10$ s. The  
 654 structure is assumed to be subjected to earthquake motion,  $f(t)$ , modeled by stationary  
 655 Gaussian white noise with spectral intensity  $S = 1 \times 10^{-2} \text{m}^2/\text{s}^3$ . The response of the  
 656 structure is computed at the discrete time instants  $\{t_k = (k - 1)\Delta t, k = 1, \dots, n_T\}$ , where  
 657 the time step size is assumed to be  $\Delta t = 0.005$ s. Hence, the number of time instants is  
 658  $n_T = T/\Delta t + 1 = 2001$ . The stochastic excitation  $f(t)$  is characterized by a sequence  
 659 of independent standard normal random variables  $\{\Xi_k, k = 1, \dots, n_T\}$  that generate the  
 660 white noise at the discrete time instants, i.e.,  $\left\{f(t_k) = \sqrt{2\pi S/\Delta t}\Xi_k, k = 1, \dots, n_T\right\}$ . The  
 661 reliability is predicted for two response thresholds,  $h^* = 0.030$ m and  $h^* = 0.035$ m.

662 In this example, there is a total of  $n_\theta = n_T + 4 = 2005$  random parameters, of which four  
 663 parameters (two stiffness parameters  $\alpha_1$  and  $\alpha_2$  and two mass parameters  $\alpha_3$  and  $\alpha_4$ ) are  
 664 updated. Using noisy simulated response time histories, the identified natural frequencies  
 665 are  $\tilde{f}_1 = 3.13$ Hz and  $\tilde{f}_2 = 9.83$ Hz, which are used as the data  $\mathbf{d}$  in the updating. We  
 666 evaluate the posterior probability of failure according to the procedure described in Section  
 667 4.4.  $\Theta_B = \{\alpha_1, \alpha_2, \alpha_3, \alpha_4\}$  are the random variables that are updated based on the  
 668 data, and  $\Theta_A = \{\Xi_1, \dots, \Xi_{n_T}\}$  are the remaining random variables characterizing the future  
 669 excitation. Using the modal data  $\mathbf{d}$ , the likelihood function for updating  $\Theta_B$  is formulated  
 670 as [42]

$$L(\theta_B|\mathbf{d}) = \exp\left(-\frac{1}{2\epsilon^2} \sum_{j=1}^2 \lambda_j^2 \left[\frac{f_j^2(\theta_B)}{\tilde{f}_j^2} - 1\right]^2\right), \quad (51)$$

671 where  $\lambda_1 = \lambda_2 = 1$  are the means and  $\epsilon = \frac{1}{16}$  is the standard deviation of the prediction

672 error between each  $\tilde{f}_j^2$  and the corresponding model squared frequency  $f_j^2(\boldsymbol{\theta}_B)$ .

673 We select a two-component Gaussian mixture (GM) model as the parametric density  
 674 family. In the present example, where the number of uncertain structural parameters to be  
 675 updated is 4, a two-component GM distribution is described by 29 unknown parameters that  
 676 are determined by CE optimization. The parametric IS density  $q_{\boldsymbol{\Theta}_B}(\boldsymbol{\theta}_B; \hat{\boldsymbol{\nu}}_{L_1})$  for evaluating  
 677 the marginal likelihood and approximating the posterior PDF of  $\boldsymbol{\Theta}_B$  is constructed based  
 678 on the procedure in Section 3. The parametric density  $q_{\boldsymbol{\Theta}_B}(\boldsymbol{\theta}_B; \hat{\boldsymbol{\nu}}_{L_2+L_1})$  approximating the  
 679 optimal IS density of the posterior probability of failure is constructed by applying the  
 680 multi-level CE method on the distribution sequence in Eq. (34), according to the procedure  
 681 outlined in [24]. Fig. 6 shows the samples of  $\boldsymbol{\Theta}_B$  obtained from the fitted parametric  
 682 densities. The four components of the samples are shown in two groups:  $\alpha_1$  versus  $\alpha_2$  in the  
 683 first column and  $\alpha_3$  versus  $\alpha_4$  in the second column of Fig. 6. The posterior joint distribution  
 684 of the stiffness parameters is bimodal, however, only one of the modes contributes to first-  
 685 passage failure. For the mass parameters, there is no significant change between the posterior  
 686 density and the optimal IS density over the failure domain. In both cases, the distribution of  
 687 the samples obtained from the parametric densities fitted through the CE method compare  
 688 well with the reference solution obtained through rejection sampling.

689 We vary the number of samples per level,  $N$ , during CE optimization between 250 and  
 690 1000. Fig. 7 shows the computational effort needed to fit the parametric IS densities  
 691  $q_{\boldsymbol{\Theta}_B}(\boldsymbol{\theta}_B; \hat{\boldsymbol{\nu}}_{L_1})$  and  $q_{\boldsymbol{\Theta}_B}(\boldsymbol{\theta}_B; \hat{\boldsymbol{\nu}}_{L_2+L_1})$  by CE optimization. The required optimization effort,  
 692 i.e., the number of samples  $N_{\text{CE},1}$  and  $N_{\text{CE},2}$ , indicates a marginal decrease in the number of  
 693 levels to convergence for increasing  $N$ , which is attributed to the larger number of effective  
 694 samples available to fit the parametric densities. We observe that the computational effort  
 695 for constructing  $q_{\boldsymbol{\Theta}_B}(\boldsymbol{\theta}_B; \hat{\boldsymbol{\nu}}_{L_2+L_1})$  is larger for the higher threshold level  $h^*$ , as the failure  
 696 event under the posterior probability measure gets rarer with increase in  $h^*$ . This leads to  
 697 an increase in the number of levels required to estimate the optimal parameters of the IS  
 698 density that best describe the failure domain.

699 The posterior first-passage probability of failure is evaluated based on the IS estimator  
 700 in Eq. (37), wherein the IS density  $q_{\boldsymbol{\Theta}_A|\boldsymbol{\Theta}_B=\boldsymbol{\theta}_B}(\boldsymbol{\theta}_A)$  of  $\boldsymbol{\Theta}_A$  is selected as suggested in [2]. The  
 701 results of reliability estimation are reported in Table 5. The simulation results are obtained  
 702 based on IS densities constructed with  $N = 500$  samples per level during CE optimization.  
 703 The estimates from the adaptive variant of the IS estimator correspond to  $\delta^* = 0.10$  and  
 704  $0.05$ . The reference solution, evaluated based on  $5 \times 10^7$  samples obtained through rejection  
 705 sampling, is  $1.85 \times 10^{-4}$  (CoV  $\approx 1\%$ ) for  $h^* = 0.030\text{m}$  and  $4.52 \times 10^{-6}$  (CoV  $\approx 6.7\%$ ) for  
 706  $h^* = 0.035\text{m}$ . The estimates of the marginal likelihood and posterior failure probability  
 707 obtained through CEIS-RelUp compare well with the reference value for both response  
 708 thresholds. For a higher  $h^*$ , there is an increase in the sample CoV of the posterior failure  
 709 probability estimates. This is due to an increase in variability of the estimator  $\hat{P}_2$  with the  
 710 threshold level. When the sample size of the IS estimators is fixed, i.e., for  $N_{\text{IS-NonAdap}}$ ,  
 711 the sample estimate  $\hat{\delta}_2$  of the CoV of  $\hat{P}_2$  is larger for  $h^* = 0.035\text{m}$ . When the sample size is  
 712 selected adaptively to meet a prescribed target CoV,  $\hat{P}_2$  requires more samples to converge  
 713 for a higher response threshold, as indicated by the larger values of  $N_{\text{IS},2}$  for  $h^* = 0.035\text{m}$ .

714 We investigate the effect of the number of samples per level during CE optimization

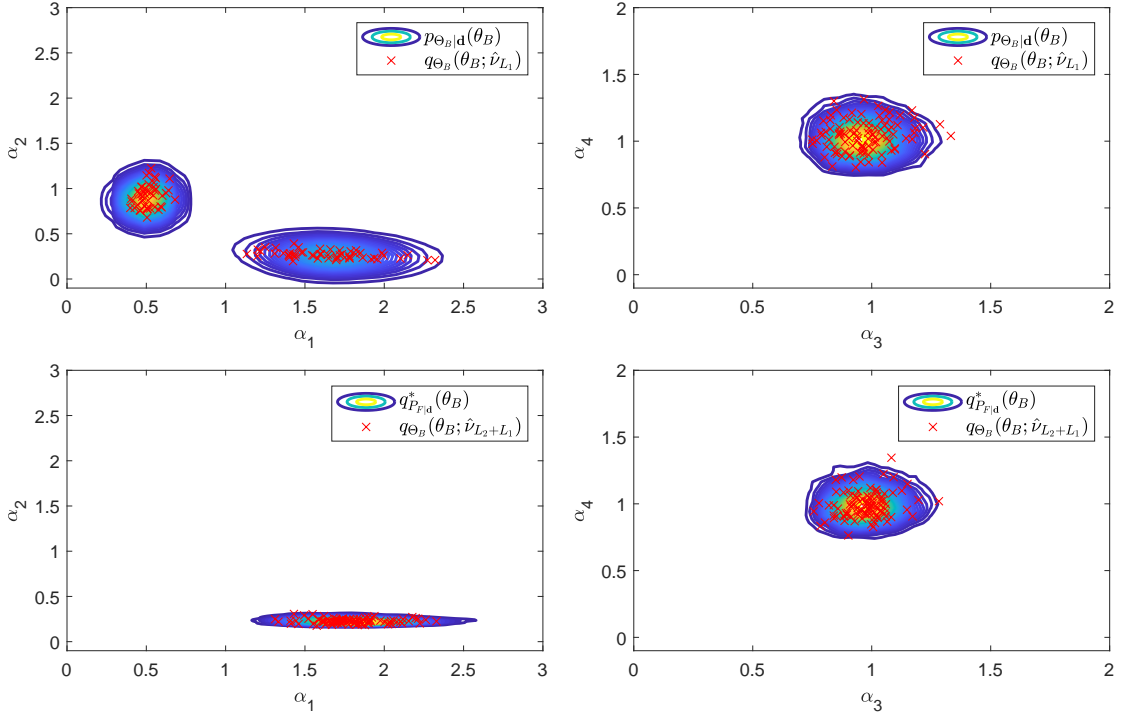


Figure 6: Samples of the stiffness parameters  $\alpha_1$  and  $\alpha_2$  and mass parameters  $\alpha_3$  and  $\alpha_4$ . Top: Joint posterior PDF of the parameters. Bottom: Joint optimal IS density over the failure domain. Scattered points denote samples from the parametric densities fitted by the CE method. Solid lines denote contours of the joint PDFs constructed based on samples obtained through rejection sampling.

715 on the performance of CEIS-RelUp. For different values of  $N$ , the sample mean of the  
716 posterior first-passage probability estimates are similar to the values in Table 5, and hence  
717 are not reported. Fig. 8 shows the variation in the sample CoV of the failure probability  
718 estimates and the total computational effort with  $N$ . For  $N_{\text{IS-NonAdap}}$ , it is observed that  
719 the sample CoV  $\hat{\delta}$  decreases with increasing  $N$ . However, once the parameters of the IS  
720 density become sufficiently optimal for larger values of  $N$ , the rate of decrease reduces. For  
721 sufficiently large  $N$ , the variation of the parameters of the fitted IS density becomes small  
722 and the rate of decrease is proportional to  $1/\sqrt{N}$  (cf. Proposition 2). This is because in  
723 the non-adaptive variant,  $N$  samples are used for estimation. The estimates of the sample  
724 CoV with  $N_{\text{IS-Adap}}$  closely adhere to the prescribed target, except for  $N = 250$  where we  
725 observe higher variability in the estimates. This is attributed to the sub-optimality in the  
726 parameters of the IS density due to the inadequate number of effective samples available  
727 for fitting the parametric density with  $N = 250$ . The total computational effort shows that  
728 selecting the sample size of the IS estimators adaptively is more efficient. For  $h^* = 0.03\text{m}$   
729 and  $h^* = 0.035\text{m}$ ,  $N_{\text{IS-NonAdap}}$  requires  $N_{\text{T}} = 6870$  and  $N_{\text{T}} = 7125$  samples, respectively,  
730 to achieve a sample CoV of 5% of the failure probability estimates. With  $N_{\text{IS-Adap}}$ , the

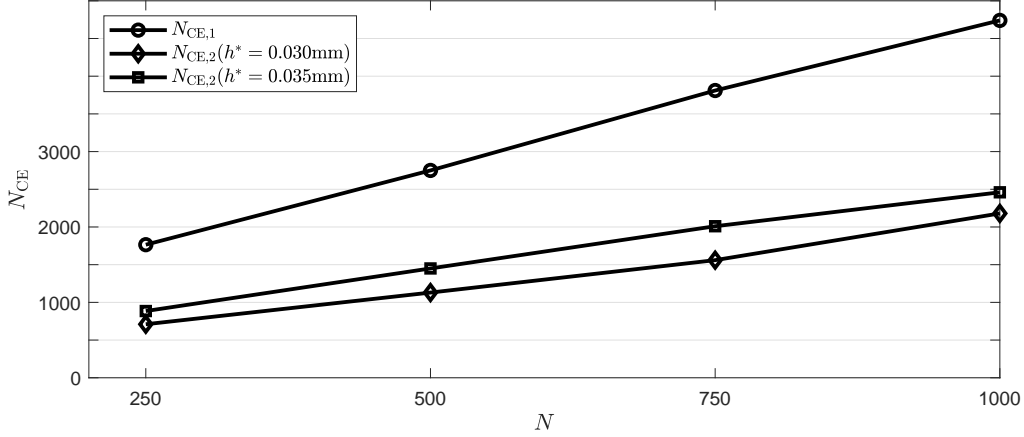


Figure 7: Cross entropy optimization effort for two-story moment-resisting frame

Table 5: Posterior first-passage probability estimates of two-story moment-resisting frame by CEIS-RelUp. CE optimization performed using  $N = 500$  samples per level. Reference value of the posterior first-passage probability, based on  $5 \times 10^7$  samples obtained through rejection sampling, is  $1.85 \times 10^{-4}$  and  $4.52 \times 10^{-6}$  for  $h^* = 0.030\text{m}$  and  $h^* = 0.035\text{m}$ , respectively. Reference value of the marginal likelihood is  $1.42 \times 10^{-3}$ .

		$\hat{c}_E$	$\hat{P}_{F \mathbf{d}}$	$\hat{\delta}$	$\hat{\delta}_1$	$\hat{\delta}_2$	$N_{IS,1}$	$N_{IS,2}$	$N_T$
$h^* = 0.030\text{m}$	$N_{IS}\text{-NonAdap}$	$1.43 \times 10^{-3}$	$1.81 \times 10^{-4}$	0.07	0.04	0.06	500	500	4880
	$N_{IS}\text{-Adap} (\delta^* = 0.10)$	$1.39 \times 10^{-3}$	$1.88 \times 10^{-4}$	0.10	0.06	0.07	98	155	4133
	$N_{IS}\text{-Adap} (\delta^* = 0.05)$	$1.42 \times 10^{-3}$	$1.81 \times 10^{-4}$	0.04	0.03	0.03	640	688	5208
$h^* = 0.035\text{m}$	$N_{IS}\text{-NonAdap}$	$1.43 \times 10^{-3}$	$4.67 \times 10^{-6}$	0.13	0.04	0.11	500	500	5200
	$N_{IS}\text{-Adap} (\delta^* = 0.10)$	$1.39 \times 10^{-3}$	$4.56 \times 10^{-6}$	0.10	0.06	0.06	98	182	4480
	$N_{IS}\text{-Adap} (\delta^* = 0.05)$	$1.42 \times 10^{-3}$	$4.68 \times 10^{-6}$	0.05	0.04	0.04	640	806	5646

731 same is achieved with  $N_T = 5208$  samples for  $h^* = 0.03\text{m}$  and  $N_T = 5646$  for  $h^* = 0.035\text{m}$ .

## 732 7. Concluding remarks

733 This contribution proposes a novel importance sampling (IS) method to update the  
734 failure probability of engineering systems based on data. An effective IS density of the  
735 uncertain model parameters is introduced to estimate the marginal likelihood of the data.  
736 The IS density is determined by minimizing the cross entropy (CE) between the posterior  
737 probability density function (PDF) of the uncertain parameters and a chosen parametric  
738 family of probability distributions. The IS density for marginal likelihood estimation leads to  
739 a sample-based approximation of the posterior PDF, which is subsequently used as a building  
740 block to construct an efficient IS density for estimating the posterior failure probability  
741 through a second round of CE minimization. The novel contribution lies in the development  
742 of a two-step adaptive multi-level approach to efficiently solve the two CE optimization

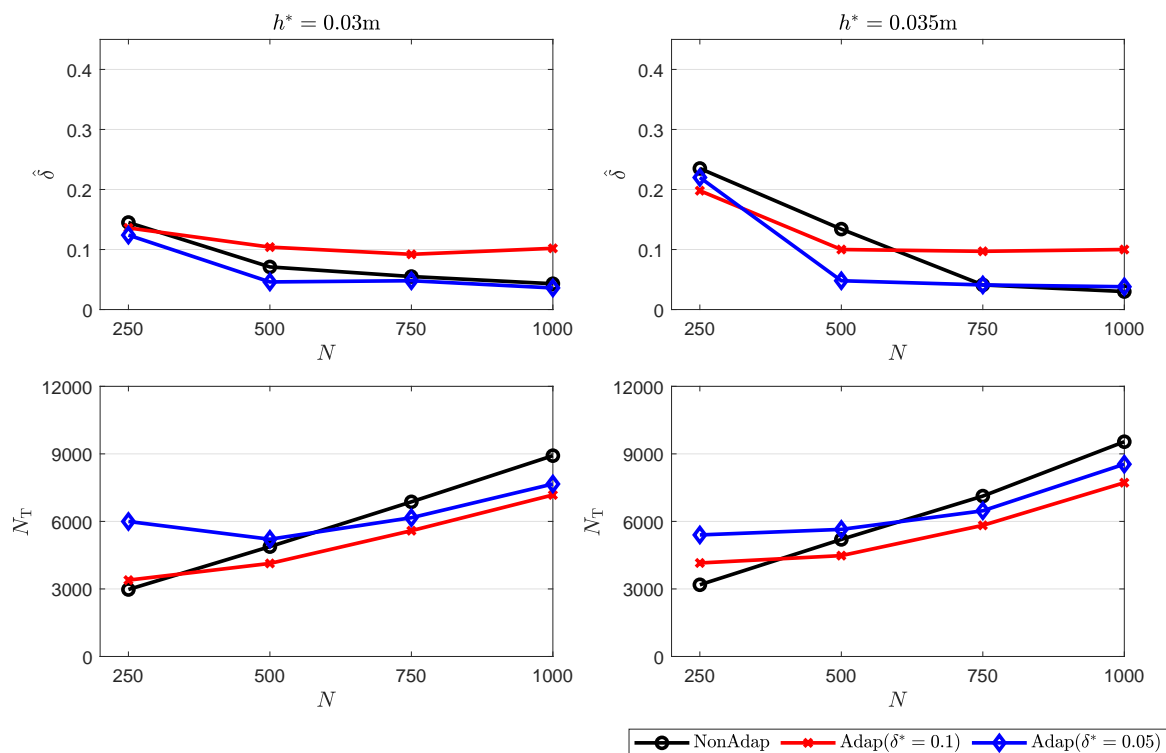


Figure 8: Coefficient of variation of posterior first-passage probability estimates and total computational effort for two-story moment-resisting frame

743 problems. Numerical studies on a range of engineering problems demonstrate that the  
 744 proposed method gives accurate estimates of the updated reliability with reasonable total  
 745 number of samples.

746 We discuss two approaches to select the sample size of the IS estimator for the posterior  
 747 probability of failure. In the first approach, the number of samples is fixed to a certain  
 748 value. The second approach considers selecting the sample size adaptively to ensure that an  
 749 estimate of the sample CoV of the IS estimator adheres to a specified target. Results from  
 750 numerical studies demonstrate that the adaptive variant of the estimator is more efficient.

751 The performance of the CE method depends on the choice of the parametric density.  
 752 We consider the Gaussian density and Gaussian mixture (GM) as the parametric families,  
 753 which are able to adequately represent a wide range of posterior distributions. However, the  
 754 number of distribution parameters to be learnt by CE optimization increases quadratically  
 755 with the number of uncertain model parameters. In an ongoing work, we explore sparse  
 756 learning approaches to accelerate the learning and improve the efficiency of the method in  
 757 high dimensions. In the numerical studies, the number of the terms in the GM model is  
 758 chosen prior to the simulation. We intend to explore adaptive approaches that estimate the  
 759 number of GM terms on the fly during CE optimization.

760 **Acknowledgements**

761 This work was supported by the Alexander von Humboldt Foundation.

762 **References**

- 763 [1] S. K. Au and J. L. Beck. Estimation of small failure probabilities in high dimensions by subset  
764 simulation. *Probabilistic Engineering Mechanics*, 16(4):263–277, 2001.
- 765 [2] S. K. Au and J. L. Beck. First excursion probabilities for linear systems by very efficient importance  
766 sampling. *Probabilistic Engineering Mechanics*, 16(3):193–207, 2001.
- 767 [3] S. K. Au and J. L. Beck. Importance sampling in high dimensions. *Structural Safety*, 25(2):139–163,  
768 2003.
- 769 [4] S. Bansal and S. H. Cheung. A new stochastic simulation algorithm for updating robust reliability  
770 of linear structural dynamic systems subjected to future Gaussian excitations. *Computer Methods in  
771 Applied Mechanics and Engineering*, 326:481–504, 2017.
- 772 [5] J. L. Beck and S. K. Au. Bayesian updating of structural models and reliability using Markov chain  
773 Monte Carlo simulation. *ASCE Journal of Engineering Mechanics*, 128(4):380–391, 2002.
- 774 [6] S. H. Cheung and S. Bansal. A new Gibbs sampling based algorithm for Bayesian model updating with  
775 incomplete complex modal data. *Mechanical Systems and Signal Processing*, 92:156–172, 2017.
- 776 [7] J. Ching and J. Beck. Real-time reliability estimation for serviceability limit states in structures with  
777 uncertain dynamic excitation and incomplete output data. *Probabilistic Engineering Mechanics*, 22(1):  
778 50–62, 2007.
- 779 [8] J. Ching and Y. C. Chen. Transitional Markov chain Monte Carlo method for Bayesian model updating,  
780 model class selection, and model averaging. *ASCE Journal of Engineering Mechanics*, 133(7):816–832,  
781 2007.
- 782 [9] J. Ching and Y. H. Hsieh. Updating reliability of instrumented geotechnical systems via simple Monte  
783 Carlo simulation. *Journal of GeoEngineering*, 1(2):71–78, 2006.
- 784 [10] P. Del Moral, A. Doucet, and A. Jasra. Sequential Monte Carlo samplers. *Journal of the Royal  
785 Statistical Society: Series B (Statistical Methodology)*, 68(3):411–436, 2006.
- 786 [11] A. Der Kiureghian and O. Ditlevsen. Aleatory or epistemic? does it matter? *Structural Safety*, 31(2):  
787 105–112, 2009.
- 788 [12] A. Der Kiureghian and P. L. Liu. Structural reliability under incomplete probability information. *ASCE  
789 Journal of Engineering Mechanics*, 112(1):85–104, 1986.
- 790 [13] O. Ditlevsen and H. O. Madsen. *Structural Reliability Methods*, volume 178. Wiley New York, 1996.
- 791 [14] M. Ehre, I. Papaioannou, K. E. Willcox, and D. Straub. Conditional reliability analysis in high dimen-  
792 sions based on controlled mixture importance sampling and information reuse. *Computer Methods in  
793 Applied Mechanics and Engineering*, 381:113826, 2021.
- 794 [15] M. Engel, O. Kanjilal, I. Papaioannou, and D. Straub. Bayesian updating and maximum likeli-  
795 hood estimation by cross entropy-based importance sampling. *Under review, Preprint available at  
796 <http://go.tum.de/808237>*, 2021.
- 797 [16] M. H. Faber. On the treatment of uncertainties and probabilities in engineering decision analysis.  
798 *Journal of Offshore Mechanics and Arctic Engineering*, 127:243–248, 2005.
- 799 [17] S. Geyer, I. Papaioannou, and D. Straub. Cross entropy-based importance sampling using Gaussian  
800 densities revisited. *Structural Safety*, 76:15–27, 2019.
- 801 [18] D. Griffiths, J. Huang, and G. A. Fenton. Probabilistic infinite slope analysis. *Computers and Geotech-  
802 nics*, 38(4):577–584, 2011.
- 803 [19] P. E. Hadjidoukas, P. Angelikopoulos, C. Papadimitriou, and P. Koumoutsakos.  $\pi 4u$ : A high perfor-  
804 mance computing framework for Bayesian uncertainty quantification of complex models. *Journal of  
805 Computational Physics*, 284:1–21, 2015.
- 806 [20] M. Hohenbichler and R. Rackwitz. Non-normal dependent vectors in structural safety. *ASCE Journal  
807 of the Engineering Mechanics Division*, 107(6):1227–1238, 1981.

- 808 [21] H. Jensen, C. Vergara, C. Papadimitriou, and E. Millas. The use of updated robust reliability measures  
809 in stochastic dynamical systems. *Computer Methods in Applied Mechanics and Engineering*, 267:293–  
810 317, 2013.
- 811 [22] S. H. Jiang and J. Huang. Modeling of non-stationary random field of undrained shear strength of soil  
812 for slope reliability analysis. *Soils and Foundations*, 58(1):185–198, 2018.
- 813 [23] S. H. Jiang, I. Papaioannou, and D. Straub. Bayesian updating of slope reliability in spatially variable  
814 soils with in-situ measurements. *Engineering Geology*, 239:310–320, 2018.
- 815 [24] O. Kanjilal, I. Papaioannou, and D. Straub. Cross entropy-based importance sampling for first-passage  
816 probability estimation of randomly excited linear structures with parameter uncertainty. *Structural  
817 Safety*, 91:102090, 2021.
- 818 [25] O. Kanjilal, I. Papaioannou, and D. Straub. Series system reliability of uncertain linear structures  
819 under Gaussian excitation by cross entropy-based importance sampling. *ASCE Journal of Engineering  
820 Mechanics*, 148(1):04021136, 2021.
- 821 [26] L. S. Katafygiotis and K. M. Zuev. Geometric insight into the challenges of solving high-dimensional  
822 reliability problems. *Probabilistic Engineering Mechanics*, 23(2-3):208–218, 2008.
- 823 [27] N. Kurtz and J. Song. Cross entropy-based adaptive importance sampling using Gaussian mixture.  
824 *Structural Safety*, 42:35–44, 2013.
- 825 [28] M. Lemaire. *Structural Reliability*. John Wiley & Sons, 2013.
- 826 [29] M. Macke and C. Bucher. Importance sampling for randomly excited dynamical systems. *Journal of  
827 Sound and Vibration*, 268(2):269–290, 2003.
- 828 [30] H. Madsen. Model updating in reliability theory. *ICASP 5, Int. Conf. on Appl. of Statistics and Prob.  
829 in Soil and Struct*, pages 565–577, 1987.
- 830 [31] R. M. Neal. Annealed importance sampling. *Statistics and Computing*, 11(2):125–139, 2001.
- 831 [32] C. Papadimitriou, J. L. Beck, and L. S. Katafygiotis. Updating robust reliability using structural test  
832 data. *Probabilistic Engineering Mechanics*, 16(2):103–113, 2001.
- 833 [33] I. Papaioannou and D. Straub. Reliability updating in geotechnical engineering including spatial vari-  
834 ability of soil. *Computers and Geotechnics*, 42:44–51, 2012.
- 835 [34] I. Papaioannou, C. Papadimitriou, and D. Straub. Sequential importance sampling for structural  
836 reliability analysis. *Structural Safety*, 62:66–75, 2016.
- 837 [35] I. Papaioannou, S. Geyer, and D. Straub. Improved cross entropy-based importance sampling with a  
838 flexible mixture model. *Reliability Engineering & System Safety*, 191:106564, 2019.
- 839 [36] R. Y. Rubinstein and D. P. Kroese. *Simulation and the Monte Carlo method*, volume 10. John Wiley  
840 & Sons, 2016.
- 841 [37] G. Schuëller, H. Pradlwarter, and P. S. Koutsourelakis. A critical appraisal of reliability estimation  
842 procedures for high dimensions. *Probabilistic Engineering Mechanics*, 19(4):463–474, 2004.
- 843 [38] G. I. Schuëller and H. J. Pradlwarter. Benchmark study on reliability estimation in higher dimensions  
844 of structural systems—an overview. *Structural Safety*, 29(3):167–182, 2007.
- 845 [39] D. Straub. Reliability updating with equality information. *Probabilistic Engineering Mechanics*, 26(2):  
846 254–258, 2011.
- 847 [40] D. Straub, I. Papaioannou, and W. Betz. Bayesian analysis of rare events. *Journal of Computational  
848 Physics*, 314:538–556, 2016.
- 849 [41] V. Sundar and C. Manohar. Time variant reliability model updating in instrumented dynamical systems  
850 based on Girsanov’s transformation. *International Journal of Non-Linear Mechanics*, 52:32–40, 2013.
- 851 [42] M. W. Vanik, J. L. Beck, and S. K. Au. Bayesian probabilistic approach to structural health monitoring.  
852 *Journal of Engineering Mechanics*, 126(7):738–745, 2000.
- 853 [43] Z. Wang and J. Song. Cross entropy-based adaptive importance sampling using von Mises-Fisher  
854 mixture for high dimensional reliability analysis. *Structural Safety*, 59:42–52, 2016.